MINNESOTA GEOLOGICAL SURVEY

MATT WALTON, *Director*

PETROLOGY OF SOME LOGAN DIABASE SILLS, COOK COUNTY, MINNESOTA

Norris W. Jones

***Report of Investigations* 29**

ISSN 0076-9177

UNIVERSITY OF MINNESOTA

Saint Paul - 1984

PETROLOGY OF SOME LOGAN DIABASE SILLS, COOK COUNTY, MINNESOTA

CONTENTS

ILLUSTRATIONS

TABLES

PETROLOGY OF SOME LOGAN DIABASE SILLS, COOK COUNTY, MINNESOTA

by

Norris W. Jones

ABSTRACT

Four diabase sills (Logan intrusions; middle Proterozoic; Keweenawan) between South and Birch Lakes, South Lake quadrangle, northeastern Minnesota, have the following general sequence of textural zones: lower chilled margin, lower fine-grained, medium-grained, coarse-grained, porphyry or porphyritic, upper fine-grained, and upper chilled margin.

Chilled margins contain scattered phenocrysts of plagioclase in a matrix of plagioclase, amphibole and/or biotite, quartz, and granular, acicular, or skeletal ilmenite. The fine- and medium-grained zones consist of plagioclase, augite, interstitial quartz, acicular apatite, some K-feldspar, and embayed, skeletal, or lath-shaped ilmenite; pigeonite and partially resorbed iron-rich olivine are present in some samples. Coarse-grained zones are distinguished by the abundance and variety of intergrowths between quartz and K-feldspar or sodic plagioclase; pyroxene is typically more altered than in finer grained zones. Porphyritic zones contain plagioclase phenocrysts which appear to be slightly more calcic than the matrix plagioclase; other aspects of the mineralogy are similar to the medium-grained zones. Deuteric alteration is extensive in all zones, but the intensity, distribution, and exact nature of the alteration are variable, even on the scale of a thin section.

Rock analyses for major oxides and microprobe analyses of feldspar, pyroxene, and olivine show that: (1) there is little variation in bulk or mineral chemistry in the fine- and medium-grained zones; (2) the composition of cores of groundmass plagioclase crystals is An_{45-52}, except in the coarse-grained zones in which it is An_{4-9}; phenocryst compositions range from An_{54} to An_{59}; (3) augite compositions are similar throughout, mostly in the range $Wo_{30-40}En_{35-45}Fs_{20-30}$; (4) chilled margins are notably richer in SiO_2 and poorer in CaO and alkalis than other zones; (5) coarse-grained zones are enriched in SiO_2 and alkalis, depleted in CaO and MgO, have high Fe_2O_3/FeO ratios, and contain plagioclase which is notably more sodic than other zones; (6) porphyritic zones are lower in Fe, MgO, and TiO_2 and richer in alkalis and Al_2O_3, reflecting the high percentage of plagioclase.

These data suggest emplacement of a magma containing plagioclase phenocrysts, minor assimilation of adjacent Rove Formation, concentration of plagioclase phenocrysts in the upper parts of the sills, crystallization from the margins inward with little or no gravity segregation of newly crystallizing phases, and migration of silica, alkalis, and water toward the coarse-grained zones, which were the last to solidify.

INTRODUCTION

Northeastern Minnesota is characterized by intrusive and extrusive igneous rocks of middle Proterozoic (Keweenawan) age (fig. 1). Largest in volume are the Duluth Complex (see Weiblen and Morey, 1980, for a recent summary) and the North Shore Volcanic Group (Green, 1972). Numerous smaller mafic intrusive complexes also have been delineated (Sims, 1970, and fig. 1). Age relationships of the Keweenawan rocks are given in Table 1.

The best known and most extensively exposed small intrusions are diabases which have been informally referred to as the "Logan sills" (Lawson, 1893) or the "Logan intrusives" (Grout and Schwartz, 1933). The term has been used rather loosely to describe most of the Keweenawan diabase sills and dikes in northeastern Minnesota and adjacent Ontario. However, Geul (1970) has demonstrated that all "Logan" diabases in the adjoining Thunder Bay District, Ontario, are not of the same age; he recognized two major types: (1) Early Mafic intrusions of tholeiitic diabase, and (2) younger Pigeon River intrusions of olivine diabase. The paleomagnetic data of Du Bois (1962), Palmer (1970), and

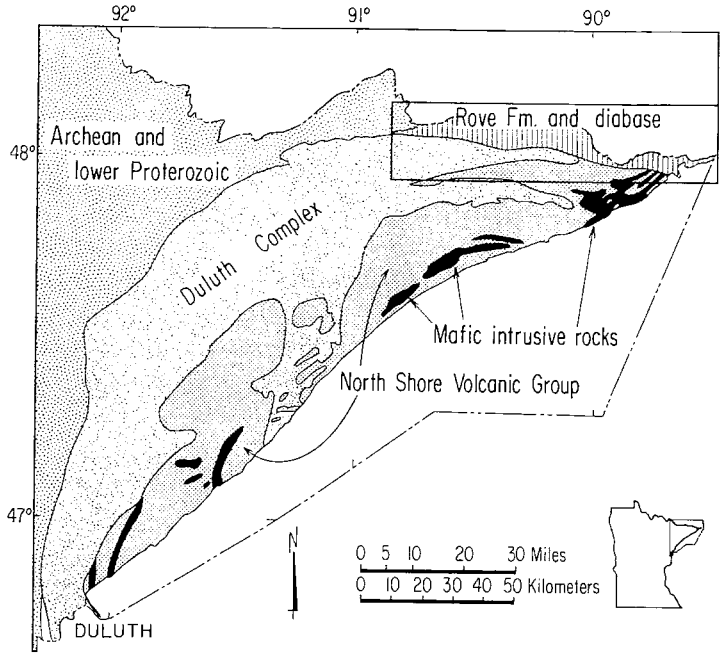

Figure 1. Generalized geologic map of northeastern Minnesota (after Sims, 1970). Most Logan intrusions are in the area labeled Rove Formation and diabase.

Table 1. Stratigraphic succession for Keweenawan rocks in northeastern Minnesota (Green, 1972; Weiblen and others, 1972; Weiblen and Morey, 1975)

	Upper Keweenawan	Hinckley Sandstone Fond du Lac Formation		
		- - - - - unconformity - - - - - - -		
Middle Proterozoic	Middle Keweenawan (normal magnetic polarity)	North Shore Volcanic Group	Duluth Complex troctolitic-gabbroic series	Pigeon River intrusions (diabase)
			?	
	Lower Keweenawan (reverse magnetic polarity)	North Shore Volcanic Group	Duluth Complex anorthositic series	Logan intrusions (diabase)
		- - - -disconformity- - - - - - - - -		
		Puckwunge Formation		
		- - - - - unconformity - - - - - - -		
Lower Proterozoic		Animikie Group	Rove Formation Gunflint Iron Formation	

Robertson and Fahrig (1971) indicate that Geul's Early Mafic intrusions have a reverse magnetic polarity, whereas the Pigeon River intrusions have a normal polarity. This, plus certain mineralogical and chemical differences, led Weiblen and others (1972) to restrict the use of the term "Logan" to the diabase intrusions having the characteristics of Geul's Early Mafic intrusions.

The Logan intrusions, as defined above, have been studied in the South Lake (Morey, 1965, 1969; Morey and Nathan, 1977), Long Island Lake (Morey and others, 1981), Gunflint Lake (Grant, 1970; Morey and Nathan, 1978), and Hungry Jack Lake (Mathez, 1971; Mathez and others, 1977) quadrangles (fig. 2).

This report focuses on four Logan sills exposed in South Lake quadrangle (fig. 2). Six weeks were spent in the field collecting samples and mapping the stratigraphy of these sills. Samples were collected at height intervals of about 3 m along one traverse through each of the sills and at other selected locations. A Jacob's staff was used to determine sill thicknesses and stratigraphic positions within sills.

Thin sections of 135 rocks were examined. Grain sizes were determined as they appeared in thin sections and average sizes were estimated; therefore, grain sizes are useful for intrasill but not intersill comparisons.

FIELD RELATIONS

The northern third of the South Lake quadrangle is characterized by east-trending hills which slope steeply to the north and gently to the south. Southward-dipping Logan diabase sills underlie the hills, and less-resistant argillite and graywacke of the Rove Formation underlie the valleys between hills. Many of the valleys contain lakes. The southern two-thirds of the quadrangle is underlain by the northern prong of the Duluth Complex, which consists of a layered series composed of 27 different units (Nathan, 1969; Morey and Nathan, 1977). Field and paleomagnetic data (Beck, 1970; Beck and Lindsley, 1969) indicate that these rocks are older than other parts of the Duluth Complex, and the layered series appears to be structurally concordant with the underlying Rove Formation and Logan sills. The quadrangle is covered with a veneer of glacial drift and is heavily wooded; rock exposures are generally small and not very abundant.

Structure

The diabase sills generally maintain their sill-like character across the entire quadrangle (figs. 3 and 4). Gentle dips of about 10° to the south are typical, but within about 0.4 km of the Duluth Complex they steepen considerably to 40° to 50° and define a monoclinal flexure as noted by Weiblen and others (1972). Sills thicken and thin laterally and up and down dip (Mathez, 1971), and branch and merge. Individual sills range in length from about 1 to 8 km, although it is generally difficult to distinguish one sill from another in the field and therefore to ascertain total length. Vertically adjacent sills generally are separated by septa of Rove Formation. Some of these septa, however, appear to thin to zero so that adjacent sills may be directly in contact with each other, although no sill-sill contacts were observed in the field because of lack of exposures.

In detail, there are deviations from an ideal sill form. The pinching and swelling implies some general discordance, and contacts having as much as 25° discordance were observed in the field.

Three small west-northwest-striking faults were noted in the field; Morey and Nathan (1977) show several northwest-striking faults as well,

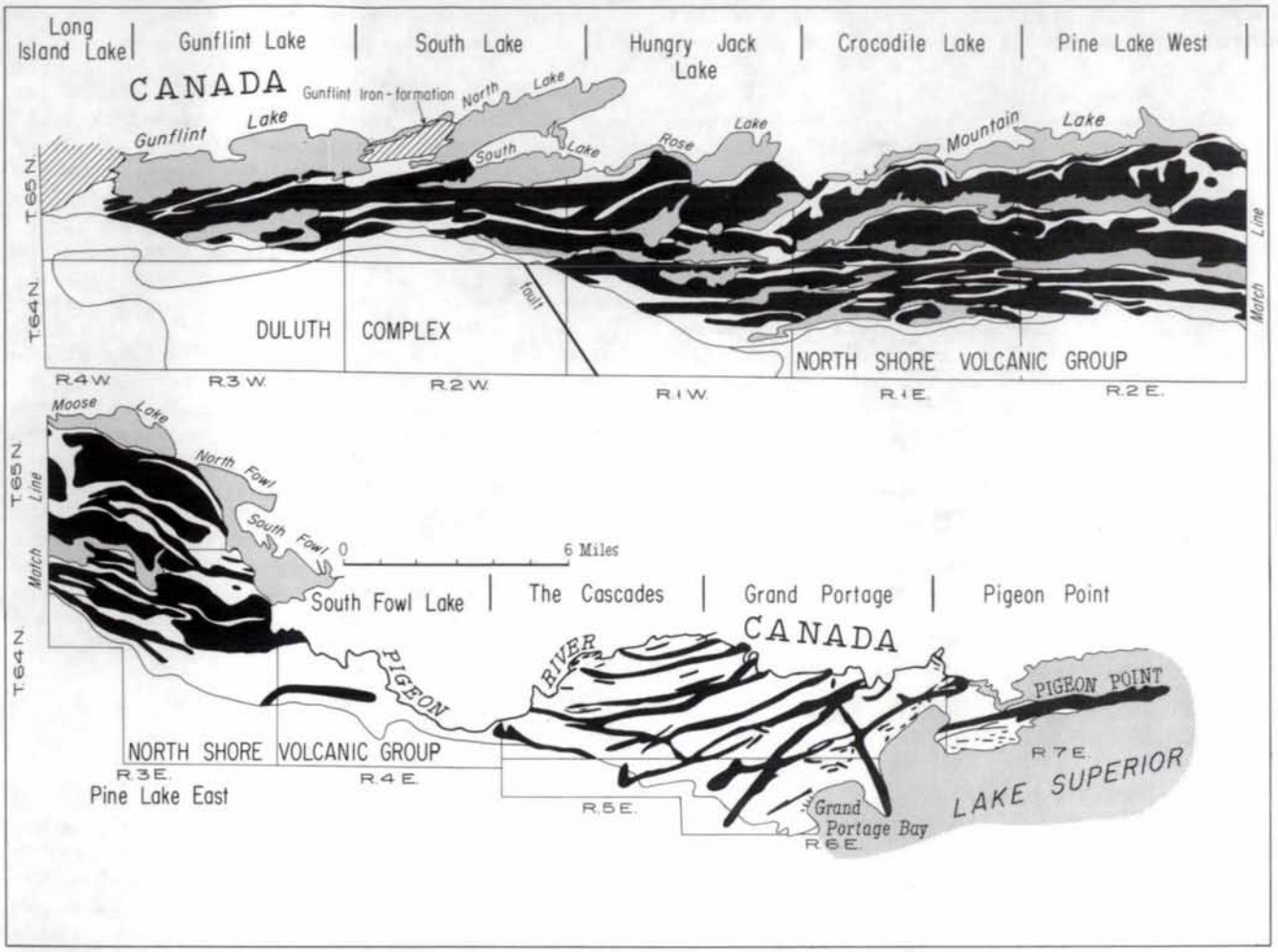

Figure 2. Distribution of diabase intrusions (black) in northern Cook County, Minnesota (after Weiblen and others, 1972). This is the area labeled Rove Formation and diabase in Figure 1.

and lineaments evident on aerial photographs indicate that there may be others. A south-side-down fault defines the contact between sills A and B in secs. 25 and 26 (fig. 3) for a short distance. The unexposed contact between these two sills is along a N. 80°-85° W.-trending valley which steepens and widens where it intersects a north-south valley roughly parallel to the section line. The base of sill B is exposed on the south side of the valley and coarse-grained diabase of sill A is exposed on the north side. A vertical basalt dike about 3 m wide, which is exposed on the north side of the valley, cuts sill A and apparently parallels the fault. A topographic depression which apparently coincides with the fault can be traced westward about 300 m before it dies out. Also south-side-down is the fault exposed in the SE1/4 sec. 26. It is a steeply dipping (85° S.) normal fault. The fault plane is characterized by a foot-wide breccia zone containing diabase fragments in a matrix of calcite and minor amounts of prehnite. The occurrence of fine-grained diabase on both sides of the fault indicates a probable displacement of less than 6 m.

The third west-northwest-striking fault is exposed just south of Sock Lake where it forms a small waterfall about 6 m high. Diabase breccia, calcite, minor pyrite, and some slickensides are present along the fault zone. Medium-grained diabase north of the fault is in contact with fine-grained diabase and Rove Formation argillite and graywacke south of the fault. The most reasonable interpretation is that the south side is upthrown with respect to the north side of the fault. Additional evidence for south-side-up movement can be seen on two prominent bluffs about 40 m south-southeast of the fault exposure. The increase in grain size from the base of the bluffs upward and the presence of fragments of Rove Formation at the base of one of the bluffs imply that the base of the sill is exposed. If there were no faulting, a sill top would be expected in this area. According to Weiblen and Morey (1975, 1980), the south sides of most east-west faults in this area are upthrown.

Sills

The four sills studied will be referred to for convenience as A-D. They correspond to the sills labeled D, E, C, and F, respectively, in Table V-34 of Weiblen and others (1972). Sill A, the longest sill studied (at least 8 km), extends from the west edge of sec. 25, T. 65 N., R. 2 W. westward along the south shore of South Lake, at least to sec. 30, T. 65 N., R. 2 W. (fig. 3). Sill B overlies sill A and is just

south of it in sec. 26, T. 65 N., R. 2 W.; it extends east-southeast across sec. 25 into sec. 36, T. 65 N., R. 2 W., a distance of about 3.4 km. Sill C is a short sill (about 1 km) south of Topper Lake (called South Round Lake on some maps). Sill D is just north of Birch Lake and the main part of it is 4.4 km long.

Textural zones were delineated in each of the sills (fig. 5) on the basis of field and thin section studies. Because of poor exposures and the gradational nature of most contacts, only the porphyritic zone of sills A and B was amenable to mapping. Its contacts are not shown on Figure 3 because of scale, but its distribution is indicated by the letter P.

Sill thicknesses and sample elevations within sills are difficult to determine because attitudes cannot be accurately determined. The dips are generally low and variations of a few degrees greatly influence the apparent thickness. For example, a sill thickness of 183 m determined using a 15° dip on either a Jacob's staff traverse perpendicular to strike or a topographic profile would be only 123 m if a 10° dip had been used.

Sill A

The thickness of sill A used in this report is 162 m, although approximate thicknesses determined from other cross sections range from 100 m to 192 m. An exposed thickness of 156 m was obtained from both Jacob's staff traverse and a topographic profile assuming a 12° dip. The total thickness of 162 m assumes that the covered top of the sill is about 6 m thick. This value was chosen by comparison with the thicknesses of the same zone in the other sills.

Samples were collected on a traverse across the sill near its apparent eastern edge, on the eastern edge of sec. 26, T. 65 N., R. 2 W. The stratigraphy illustrated in Figure 5 is based on that traverse. Only the lower contact was located on the traverse; the uppermost part of the sill is not well exposed except in the vicinity of Topper Lake.

The lateral extent of sill A was determined on the basis of topographic continuity and exposures of the diabase porphyry near the top of the sill. No porphyry was found east of the terminus indicated on Figure 3 although fine-grained diabase characteristic of this zone was located at several places north of Dunn Lake.

The thickness of the porphyry zone seems to be consistently 6 to 8 m. The best exposures are just north of Topper Lake where the lower contact is exposed on several north-facing vertical cliffs. The contact there appears to be quite abrupt although it is not sharp. It is defined by the sudden appearance of randomly oriented plagioclase phenocrysts in a matrix which appears to be much the same as the diabase just below it; in detail the contact is defined by crystal faces of the plagioclase phenocrysts.

The contact between sills A and B was observed at only two places--at the west end of sill B and at the southeast corner of sill A (fig. 3). At the west end of sill B, on the west side of a steep-sided, north-northeast-trending valley, fine-grained diabase is underlain by diabase porphyry. Dip slopes and the contact between the two units have anomalous north-south strikes, rather than east-west, and dip about 30° E. The porphyry is interpreted to be within sill A. On the east side of the valley, a fine- to medium-grained diabase exposed on a cliff strikes N. 10° E. and dips 32° E. This diabase, which is underlain at one place by Rove Formation argillite, is interpreted to belong to sill B. The strike of the contact between the two sills is about north-south here, but it must swing around to trend west-northwest, although this could not be verified in the field. The contact at the southeast corner of sill A appears to be along a fault. The fault itself is not exposed, but the lower chilled margin of sill B can be followed horizontally to within about 7 m of the coarse-grained zone of sill A; the interval between is covered. The contact shown on Figure 3 is inferred from topography and extrapolation from known contacts.

Sill B

A thickness of sill B of 77 m was determined from topographic profiles and Jacob's staff traverses, assuming a 12° dip. It was assumed that a normal fault, which cuts the upper exposed part of the sill, caused a displacement of 6 m; this 6 m is included in Figure 5 in the thickness of the fine-grained diabase zone at the top of the sill.

Samples of sill B were collected along a traverse in the general vicinity of the boundary between secs. 25 and 26. Both upper and lower contacts are exposed. The most distinctive unit in the sill is the diabase porphyry, which was used to define the lateral limits of the sill. The western end of the sill, as mentioned above, coincides with the steep north-northeast-trending valley along the boundary between secs. 26 and 27, T. 65 N., R. 2 W., where there is a small exposure of Rove Formation. The eastern end of the sill is poorly defined; its location is inferred from topography and the absence of diabase porphyry farther east. Complicating the picture is the widespread occurrence of diabase porphyry in sill B north-northwest of Hoat Lake, which requires a change in attitude of the sill. In this area, instead of dipping southward, the sill dips to the southeast at an angle roughly parallel to the slope. This change in attitude appears to be local, as it is not reflected east of the creek flowing north from Hoat Lake.

The contact between sill B and underlying Rove Formation is exposed just south of the fault on the section line between secs. 25 and 26, and is conformable to the N. 80° W., 12° S. attitude of the underlying argillite. The top of sill B is exposed just west of the stream

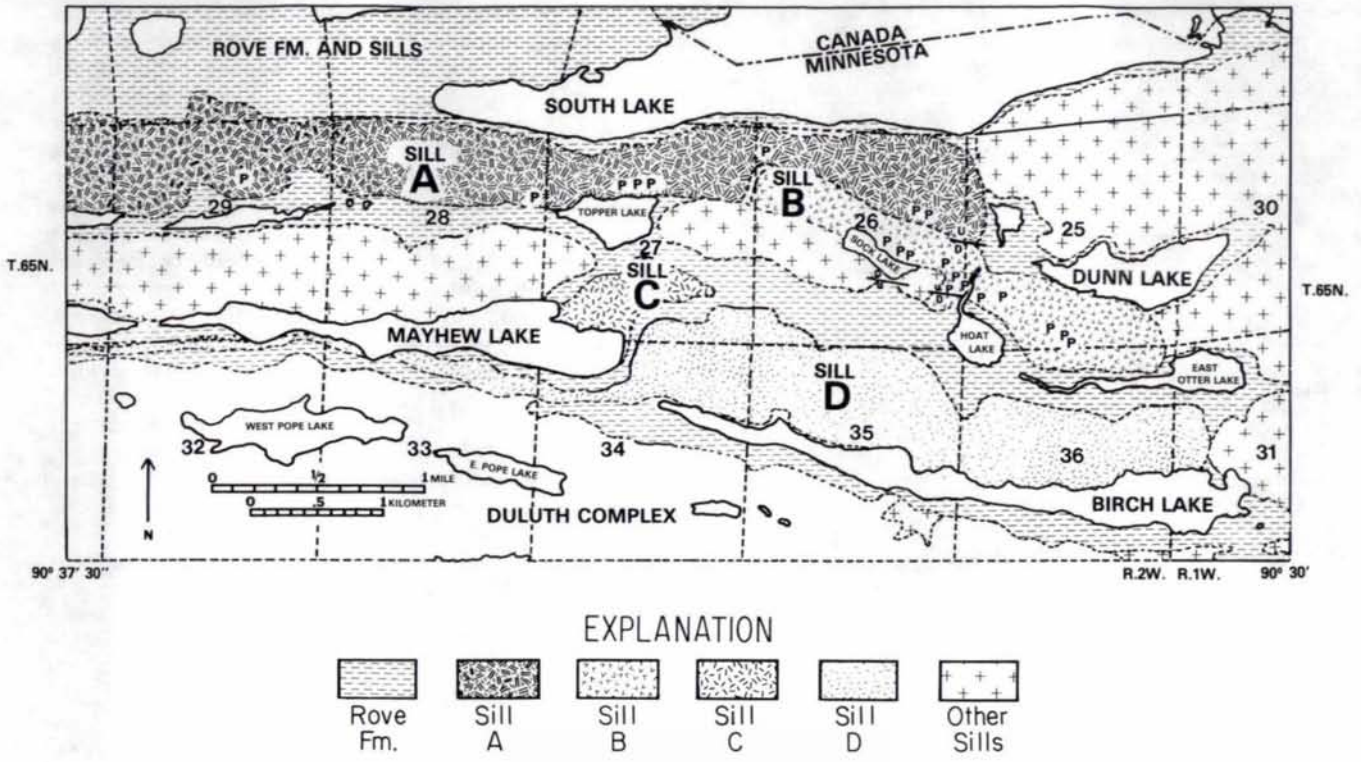

EXPLANATION

Rove Fm. | Sill A | Sill B | Sill C | Sill D | Other Sills

Figure 3. Geologic map of part of the South Lake quadrangle (modified from Morey, 1965); see Figure 2 for location; P, locations of the diabase porphyry described in the text.

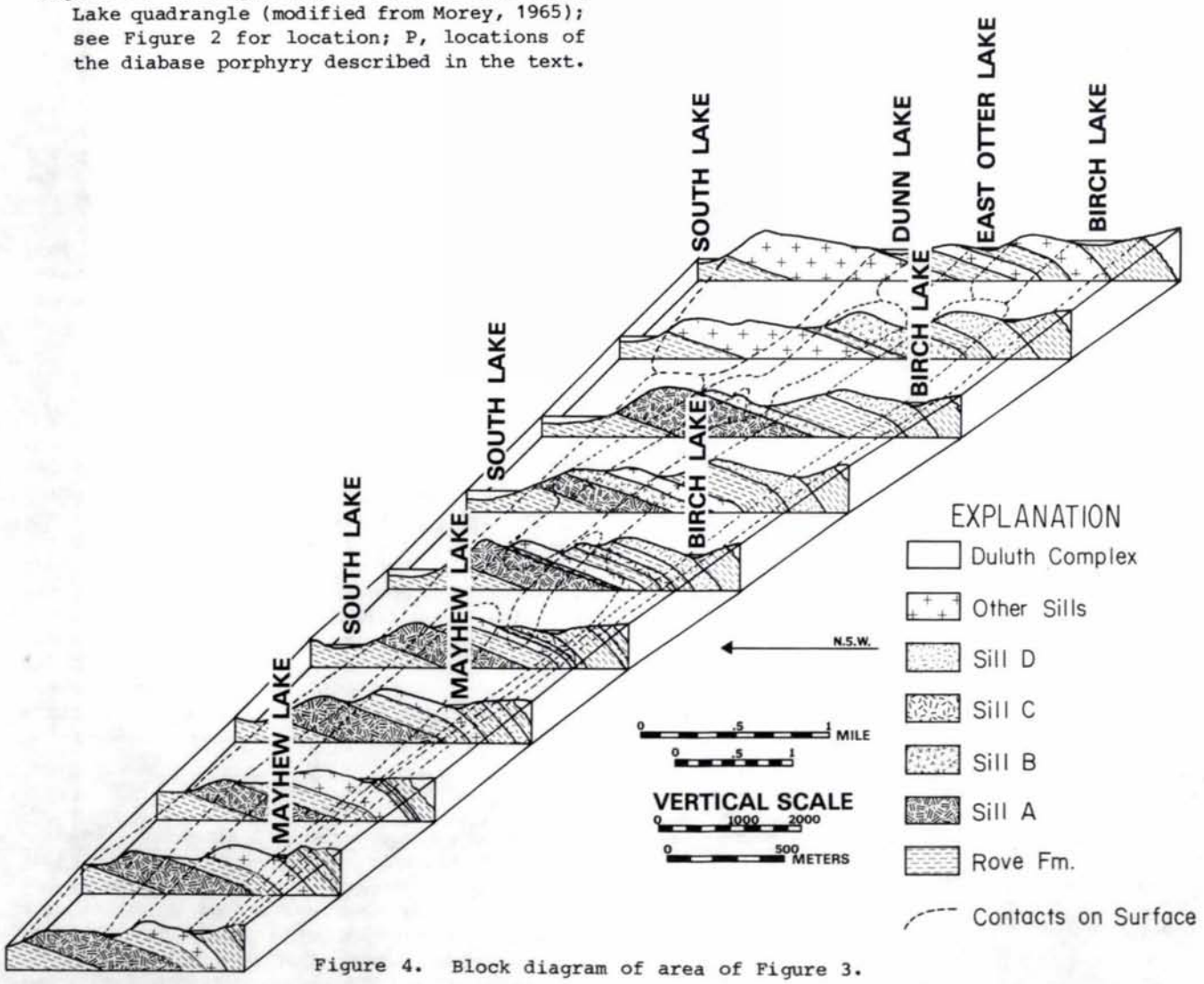

Figure 4. Block diagram of area of Figure 3.

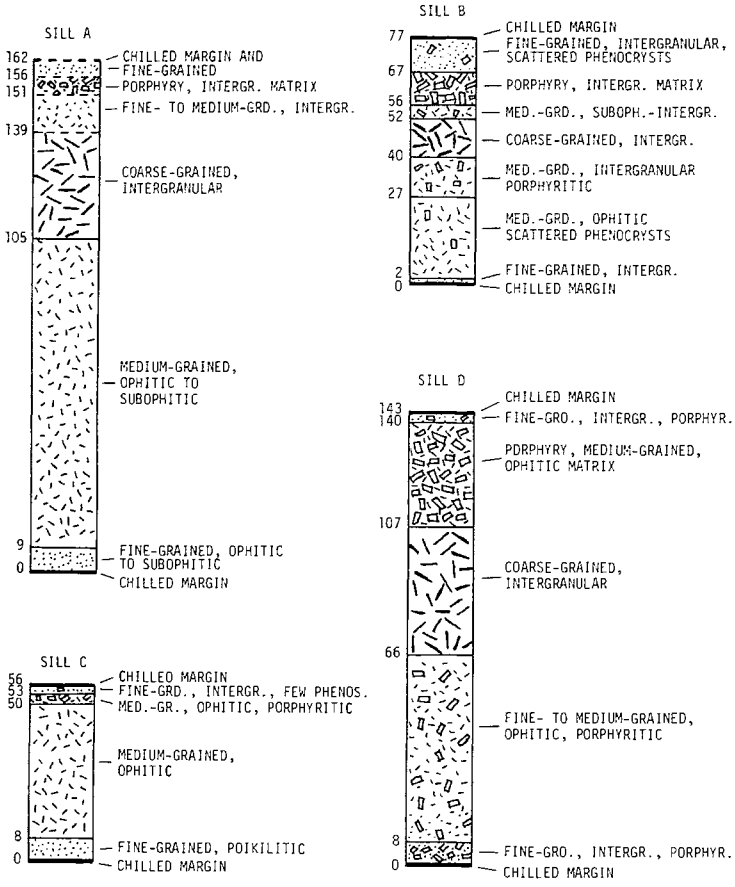

Figure 5. Stratigraphy of the four sills studied showing textural zones and heights in meters. Compare with Table 2 below.

Table 2. Fabrics observed in textural zones

Zone	Observed Fabrics
Upper chilled margin	Intergranular (sills A, B, D) Intergranular, porphyritic (sill C)
Upper fine-grained	Intergranular (sills A, C) Intergranular, porphyritic (sills B, D)
Porphyry or porphyritic	Intergranular matrix (sills A, B) Ophitic matrix (sills C, D)
Coarse-grained	Intergranular (sills A, B, D)
Medium-grained	Ophitic (sills A, C) Porphyritic and ophitic (sills B, C, D) Porphyritic and intergranular (sill B)
Lower fine-grained	Ophitic (sill A) Poikilitic (sill C) Porphyritic, intergranular (sill D) Intergranular (sill B)
Lower chilled margin	Intergranular (sill A) Intergranular, porphyritic (sills B, C, D)

flowing out of Hoat Lake and just south of the fault. Thin (less than 1 cm) remnants of Rove Formation are present, but are difficult to distinguish from chilled diabase in the field. The contact between sill B and the overlying sill south and west of Sock Lake is not exposed, but is inferred because diabase porphyry and fine-grained diabase north of Sock Lake define the top of sill B, and medium-grained diabase south of Sock Lake defines the middle part of the overlying sill. It is possible that sill B and the overlying sill are in fault contact, because the inferred contact coincides with a prominent west-northwest-trending lineament. Several traverses were made across the sill south of sill B. Its stratigraphy is (from the bottom): fine-grained diabase, medium-grained diabase, coarse-grained diabase, and fine-grained diabase.

The porphyry in sill B is identical to that in sill A. In general, both upper and lower contacts seem to parallel the upper and lower sill contacts, but locally they may be quite irregular. The lower contact in the NE¼SE¼ sec. 26, T. 65 N., R. 2 W. is quite irregular and the porphyry there ranges in thickness from 4.5 to 6 m. The underlying medium-grained diabase contains plagioclase phenocrysts 1 to 3 cm long within 0.3 m or less of the porphyry. The porphyry itself is marked by the sudden appearance of numerous plagioclase phenocrysts set in a medium-grained diabase matrix like the underlying rock. The contact is sharp in the sense that you can put your hand on it, but irregular in that it is defined in detail by the crystal boundaries of the plagioclase. The upper contact, observed just north of the south-side-down fault north-northwest of Hoat Lake (fig. 3), is similar in that the overlying diabase is porphyritic or contains scattered phenocrysts. An excellent exposure of the upper contact also occurs on the north shore of Sock Lake.

Sill C

Identical thicknesses of 56 m were obtained from sill C (fig. 5) from the Jacob's staff traverse and from a topographic profile, using a dip of 11°. Both lower and upper contacts are exposed along the line of traverse from the center of sec. 27 southward. The lower contact with Rove Formation arkose is sharp and slightly irregular. The top of the sill is well exposed along a Forest Service road; it is largely chilled diabase, but thin (less than 1 cm) patches of Rove Formation argillite can be found with careful observation. Inclusions of anorthositic gabbro and graywacke are also present.

Sill D

The thickness of sill D is especially difficult to determine because the dip increases toward the south as the Duluth Complex is approached. The lower contact on the north side of the sill dips south at 12°, but sheeting joints within 300 m of the upper contact dip more than 20° and the upper contact and adjacent

Rove Formation dip as much as 50°. It could not be determined just how this change in dip occurs. If it is assumed that the dip changes progressively in a regular fashion, the sill would be 280 m thick. Such a change, however, seems unreasonable in comparison to dip changes elsewhere in the area near the Duluth Complex. The thickness of 143 m used in this report is based on the assumption that the dip remains at 12° to within about 600 m of the Duluth Complex, and then progressively steepens to 45°.

Samples of sill D were collected along a north-south traverse through the center of the E½ sec. 35, T. 65 N., R. 2 W. Both the upper and lower contacts were located. The west end of the sill is well exposed just east of Mayhew Lake. The east end is poorly defined and its location in Figure 3 is based on topography and the apparent absence of the distinctive porphyritic zones of the lower part of the sill in diabase to the east.

The lower contact, which is difficult to distinguish because the baked Rove Formation argillite looks very much like the chilled diabase, varies from sharp and planar to somewhat irregular. The upper contact was seen at only one locality, where it exhibits about 25° of discordance. In a few exposures, a 3-m-thick texturally similar sill was observed about 3 m below sill D.

In comparison to the other sills (fig. 5), sill D has an exceptionally large proportion of phenocrysts in both upper and lower levels.

Dikes

Olivine diabase dikes were found at six locations within the study area and there are undoubtedly many others. Two dikes cut sill A along the traverse line, one with an attitude of N. 5° E., 35°-40° SE., and a thickness of 2 m, the other with an undetermined attitude and thickness. Several dikes having an attitude of about N. 85° W., 90° and a thickness of about 3 m occur long the fault contact between sills A and B. A dike several meters thick, which has an approximately east-west, 90° attitude, was found along the contact between sill B and the overlying sill in the SE¼NE¼ sec. 27. A thin dike cuts the top of sill C along a Forest Service road in sec. 27, and a thick (∿30 m) east-west dike cuts sill D in sec. 35. All of the dikes are interpreted to be age equivalents of Geul's (1970) Pigeon River intrusions.

PETROGRAPHY

Each of the four sills studied can be subdivided into several textural zones recognizable in the field or in thin section. With one exception, seven zones are common to all of the sills studied. These are: lower chilled margin, lower fine-grained zone, medium-grained zone, coarse-grained zone, diabase porphyry, upper fine-grained zone, and upper chilled margin. Average grain sizes of these zones are: chilled margins, less than 0.5 mm; fine-grained zones, 0.5-1.0 mm; medium-grained zones, 1-4 mm; and coarse-grained zones, larger than 4 mm. The four sills differ in detail in terms of fabric within each of the textural zones as outlined in Table 2. Details of grain-size variation are shown in Figure 6. Textures, mineralogy, and fabric of each zone are described below.

Lower Chilled Margins

The lower chilled margin is characterized by a very fine grained, felty, intergranular texture (fig. 7). It comprises about 1 percent of the sill and is typically 0.3 to 0.6 m thick. Poorly defined anhedral plagioclase, equant to acicular amphiboles, and branching and non-branching acicular Fe-Ti oxides are invariably present; scattered plagioclase phenocrysts and biotite are present in sills B, C, and D. Matrix plagioclase laths in this zone have average lengths of 0.04 to 0.4 mm; equant amphiboles are mostly in the range 0.02 to 0.3 mm, but acicular grains are as long as 2.1 mm. Overall average grain size is less than 0.5 mm.

Plagioclase

Matrix plagioclase occurs as diversely oriented, poorly defined anhedral laths with corroded margins, and as irregularly shaped anhedral grains. Most grains are untwinned; some albite twins having only two lamellae occur. Normal compositional zoning is indicated by the nature of the extinction, but the composition range could not be determined.

Phenocrysts of plagioclase occur as scattered (less than 5 percent) individual grains or as open clusters of several grains in sills B, C, D. They are generally tabular and subhedral to euhedral, although some grains have ragged ends and smaller grains are somewhat rounded. Most phenocrysts show albite twins and some also show combined twins (albite-Carlsbad and/or albite-pericline). Minor oscillatory zoning, evident on the outer margins of many phenocrysts, is superimposed on a normal zoning which also is typically confined to the outer 10 percent of the crystal.

Sericitization of matrix plagioclase is variable, ranging from essentially zero (sill D) to 60 percent (sill A). Phenocrysts are generally clear or contain only a few percent sericite.

Mafic Silicates

Pyroxene is either absent (sills B and C) or severely altered (sills A and D) in the chilled margins. In sill A it may occur in the matrix, but is so altered that identification is not certain; in sill D there are a few microphenocrysts (0.9 mm) of altered pyroxene.

The typical mafic silicate of the chilled margin is a pale-green amphibole which is presumed to be a hornblende ($\underline{Z} \wedge \underline{c} = 17°-20°$). In sill C the amphibole at the contact is a brown

SILL A

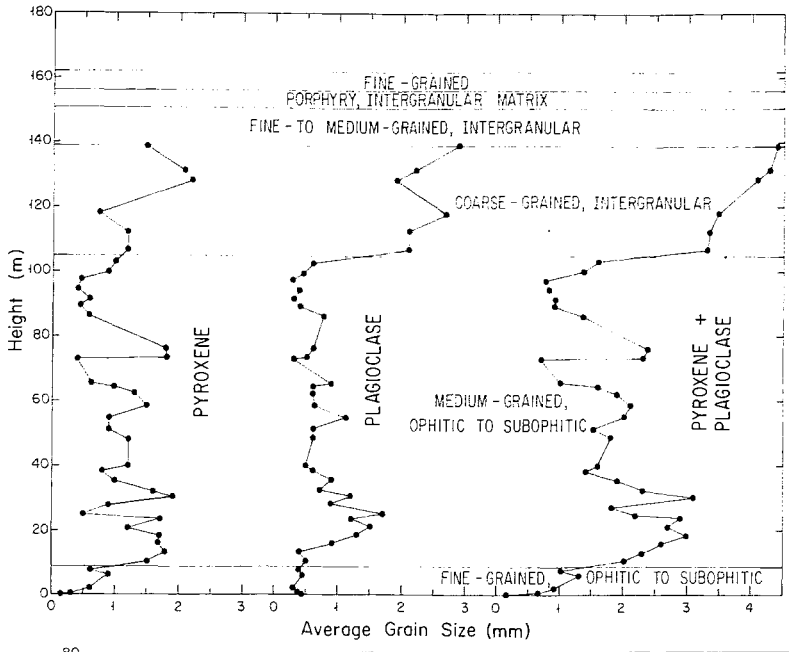

SILL B

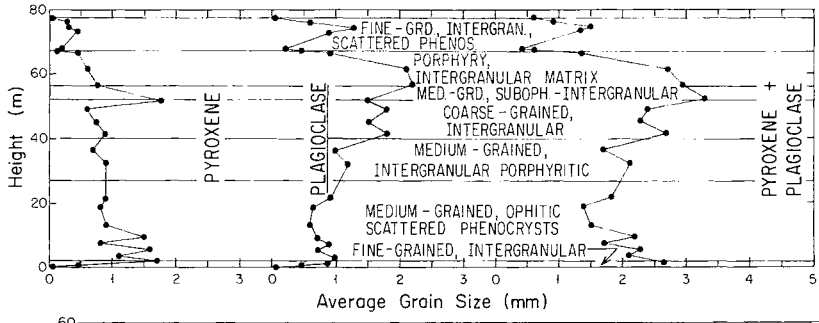

SILL C

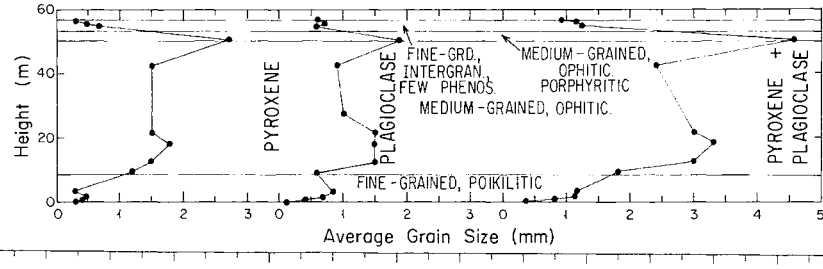

SILL D

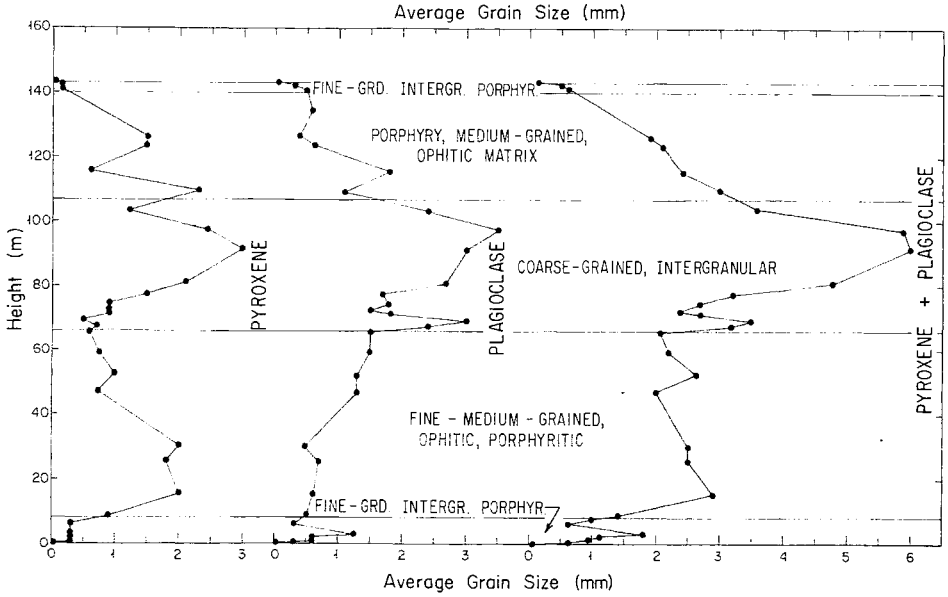

Figure 6. Variation in grain size with height in sill. Grain sizes shown for pyroxene are estimated average grain diameters observed in thin section; those for plagioclase are average lengths of laths (matrix plagioclase in porphyritic zones) observed in thin section. Pyroxene + plagioclase is simply the sum of the grain sizes of pyroxene and plagioclase and better emphasizes variations.

variety, but 0.5 m above the contact, it is green. Grain shapes vary from anhedral and irregular to elongate to acicular. In sills A and B, acicular grains with ragged margins occur in fan-shaped clusters. Amphibole grains have uneven optical extinction, and are charged with tiny (<0.01 mm) opaque inclusions; many are partly altered to biotite.

Brown biotite occurs both as discrete crystals and as grains in direct contact with amphibole. The latter form small irregular patches within amphibole or on the margins of amphibole grains, and are presumed to have been derived from it by alteration. In sill D, however, reddish-brown microphenocrysts of biotite with diameters of 0.12 to 0.21 mm and narrow (0.03 m) rims of quartz are not associated with amphibole. It is not clear whether the quartz formed by reaction between biotite and the matrix, or whether it is a byproduct of a reaction which yielded the biotite.

Opaques

The principal opaque minerals are Fe-Ti oxides, presumably ilmenite (see discussion of Fe-Ti oxides in the section on mineral chemistry). Three textural types of ilmenite were distinguished within the chilled margin: small equant grains, acicular grains, and skeletal grains. Immediately adjacent to the contact, equant grains are very much more abundant than the others, but about 2 cm from the contact, equant and acicular grains become equally abundant, and comprise at least 90 percent of the opaque grains. The small equant grains have average diameters of 0.002 to 0.04 mm; most have very ragged to embayed margins (fig. 8a), and some of the larger ones have one or two small holes. The small equant grains are either evenly disseminated throughout a thin section or somewhat concentrated in poorly defined open clusters. In general, however, they are associated with, or included in, mafic silicates.

Acicular grains (figs. 7, 8b) occur as single needles with smooth or irregular margins, as needles composed of discrete, small, irregular but rounded grains, and as needles with nodes and branches. Branches may extend from one or both sides and be normal or non-normal to the "trunk." In some needles the "trunk" appears to be missing and only the branches remain. The needles range in average length from 0.04 to 0.6 mm. In sills A, B, and C, needles occur in clusters of 10 to 15 parallel, nonbranching grains. Clusters range from more or less equant to elongate; in the latter, the direction of cluster elongation is normal to needle orientation. Needle orientation in adjacent clusters is generally different.

Skeletal grains (fig. 8c) are generally less common than equant and acicular grains. Some of the skeletal grains in sills A and B have subhedral to euhedral, triangular or square outlines, and the holes in the grains are elongate and parallel to specific crystallographic planes (presumably {111} of an isometric predecessor). Holes between the elongate solid parts of some grains are about twice as wide as the solid parts. In sills A, B, and D, skeletal crystals consisting of more or less equant open groups of intersecting branching acicular grains are present. Typical skeletal grains of this type consist of three parallel branching needles which are normal to two or three other branching needles to form a network of needles and branches which intersect at right angles.

Generally, only minor amounts of anhedral to subhedral pyrite are present in the chilled margins, but pyrite in sill C is concentrated in a zone 1 cm thick 5 cm above the base. Pyrite grains generally are larger (0.3 to 1.2 mm) than the Fe-Ti oxide grains, typically have ragged margins, and commonly have several holes.

Quartz

Anhedral, irregular-shaped, interstitial quartz is identifiable in thin sections of coarser grained rock from the chilled margins, but is difficult to distinguish from untwinned plagioclase because the grain size is generally less than 0.15 mm. Some quartz occurs in very simple intergrowths with feldspar and amphibole, but most is not intergrown. Randomly oriented needles of apatite are typically included in the quartz grains, and rare groups of parallel needles also are present. Apatite needles may extend into the adjoining feldspar.

Xenoliths

Xenoliths of quartzite from the adjacent Rove Formation were observed in the chilled margins of sill C, and Rove xenoliths presumably are present in similar positions in other sills. Adjacent to the xenoliths in one thin section, the diabase is especially fine grained and fewer Fe-Ti oxides and only equant types are present. The texture of such a mini chilled zone, which is 0.5 to 6 mm wide in thin section, is similar to the chilled margin as a whole.

Lower Fine-Grained Zones

The lower chilled margin passes imperceptibly upward into fine-grained diabase which comprises between 1 and 13 percent of the four sills studied (fig. 5). Average grain size within this zone is 0.5 to 1 mm. Each of the four sills is characterized by a different fabric within this zone.

Sill A

The lower fine-grained zone of sill A has an ophitic to subophitic texture (fig. 9a). Plagioclase laths having somewhat scalloped and rounded margins are wholly or partly enclosed in pyroxene or its alteration products. These laths average 0.3 to 0.5 mm in length, but some are as long as 1.3 mm. Plagioclase also occurs in clusters of 5 to 10 grains between the ophites, where it is commonly associated with

Figure 7. Photomicrograph of typical chilled margin. Note acicular Fe-Ti oxides and fan-shaped cluster of amphibole crystals. Sample M11556; width of view 0.9 mm, uncrossed polars.

quartz; these plagioclase grains commonly have irregular shapes, although they tend to be elongate. Twinning is more prominent in the coarser grained parts of the zone; albite twins predominate, but a few albite-Carlsbad twins occur in most thin sections. Normal compositional zoning is evident in both ophite and cluster plagioclase, and minor oscillatory zoning was also noted. The degree of sericitization ranges from nil to moderate and is variable on the scale of a thin section.

The pyroxene, a very pale tan augite with 2V ∿48°, occurs as irregularly shaped ophites which consist of either single crystals having even or uneven extinction, or composites of crystals having slightly different optical orientations. Some grains are twinned on {100}. Pyroxene is slightly to totally altered to amphibole, biotite, and some chlorite. The alteration makes it difficult to determine the grain size of original ophites, but average grain diameters appear to range from 0.6 to 0.9 mm, with largest grains to 1.6 mm.

The typical opaque oxide in this zone has an irregular shape with embayed margins, and contains rounded inclusions of silicates. A few grains are skeletal with vermicular textures, and some are lath shaped. Grain size averages 0.3 mm.

Interstitial quartz occurs in minor amounts as irregularly shaped grains; it is not intergrown with feldspar. A few rounded grains of unaltered olivine were noted in one thin section.

Sill B

Sill B has a lower fine-grained zone characterized by a poorly defined intergranular texture (fig. 9b). Plagioclase is 90-percent

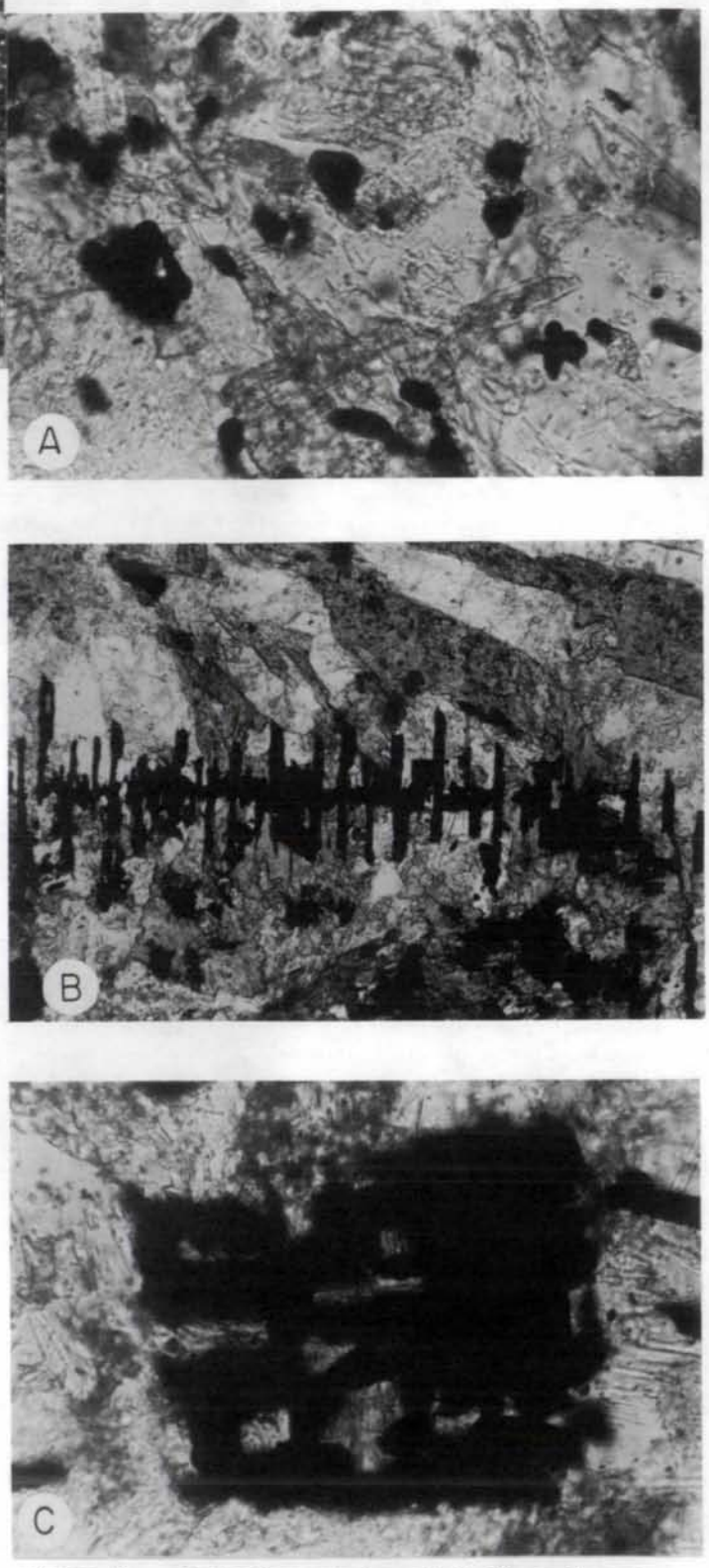

Figure 8. Photomicrographs of Fe-Ti oxides in chilled margins, uncrossed polars. A, equant grains; sample M11556; width of view 0.24 mm. B, branching acicular grain; sample M11585, width of view 0.9 mm. C, skeletal grain; fuzzy appearance is normal; sample M11517; width of view 0.24 mm.

sericitized and pyroxene has been completely uralitized so that the original texture is partly obliterated. Plagioclase grains are anhedral and most are elongate, having an average width of 0.4 mm and ranging to 2.1 mm in length; some very irregularly shaped grains appear to be interstitial. Grains are largely masked by sericite, but poorly defined albite twins are present and grains seem to be normally zoned.

Most of the amphibole, a pale-yellow and pale-green hornblende with $\underline{Z} \wedge \underline{c} = 20°$, occurs as equant but very irregularly shaped grains between grains of plagioclase. Some grains have small brown patches which are optically continuous with the rest of the grain, and most grains include tiny (<0.001 mm) grains of sphene(?). A few grains partially enclose plagioclase in a relict subophitic relationship. A few grains are as long as 3.3 mm. Equant grains of amphibole average 0.4 mm in diameter; most are single and optically continuous, but a few are composite.

Lath-shaped opaque oxides 0.3 mm long occur as groups of 10 to 15 parallel laths and as single grains. Most have slightly irregular margins, but some have small rounded branches. Embayed irregular-shaped opaque oxide grains with silicate inclusions are also present. Quartz occurs as small (0.3 mm) interstitial patches, and is associated with needles of apatite.

Sill C

Sill C is characterized by an allotriomorphic-granular to allotriomorphic-seriate texture in which most of the plagioclase poikilitically encloses pyroxene or its altered equivalent and opaque minerals (fig. 9c). This is the only sill in which this relationship was noted, but Mathez (1971) has described similar textures in the lower parts of two sills in the adjoining quadrangle to the east. In the lower part of the lower fine-grained zone, the plagioclase oikocrysts are all anhedral; some are as large as 1.8 mm in diameter, but the average diameter

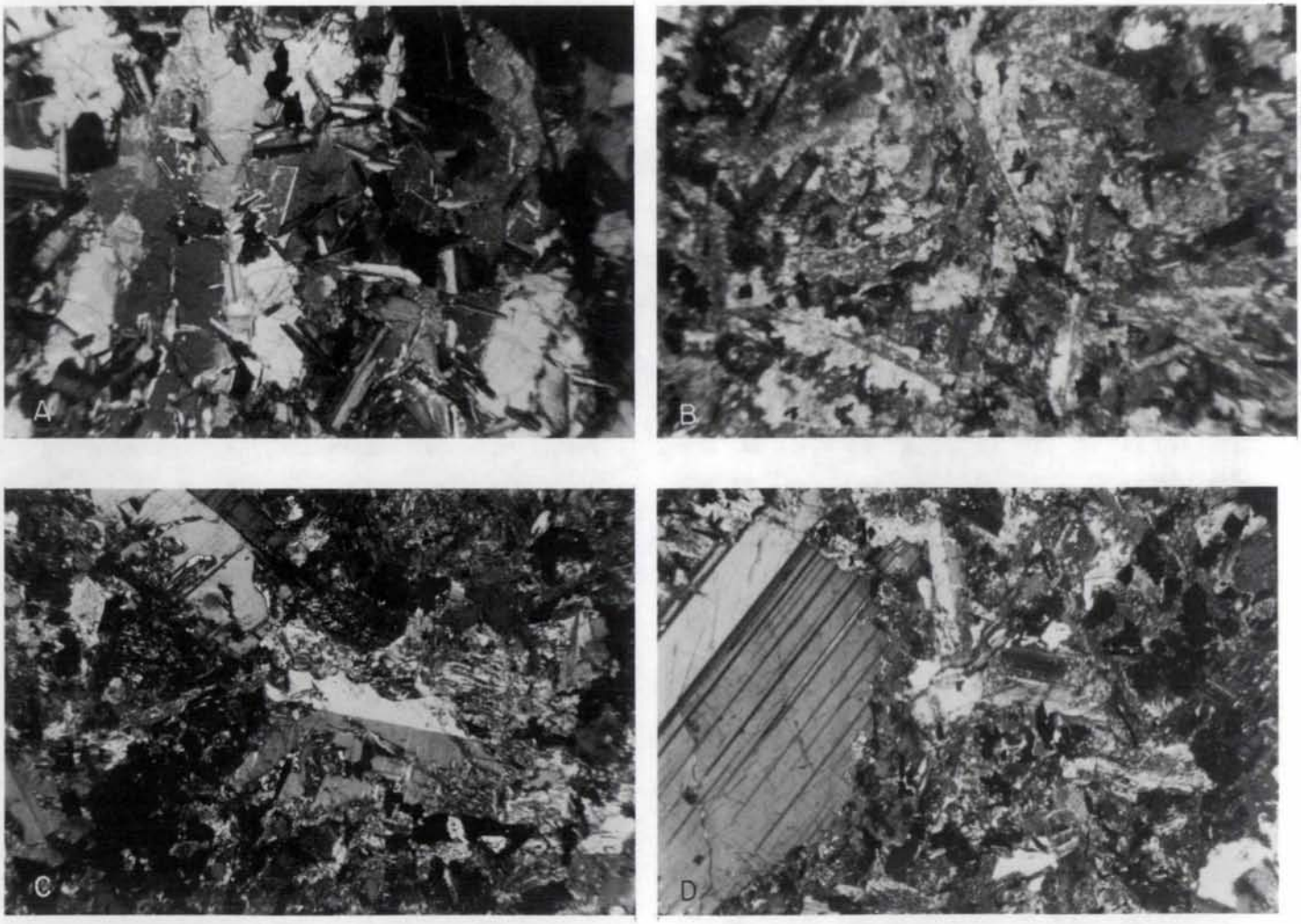

Figure 9. Textures of lower fine-grained zones; width of view 3.7 mm, crossed polars. A, ophitic texture of sill A, sample M11616. B, intergranular texture of sill B; plagioclase and pyroxene severely altered; sample M11557. C, poikilitic plagioclase enclosing augite or altered equivalent, sill C; sample M11625. D, porphyritic texture of sill D with anhedral plagioclase phenocrysts in an altered intergranular matrix; sample M11588.

is 0.7 mm. Toward the top of the zone, grains are increasingly lath shaped, having average lengths of 0.9 mm, and not all grains are poikilitic. Chadacrysts are rounded and generally less than 0.3 mm in diameter. Some plagioclase oikocrysts are so charged with chadacrysts that it is not immediately obvious that they are single optically continuous grains. Most twins are albite twins, but albite-Carlsbad and albite-pericline twins are also present. Sericitization averages 30 percent but ranges from 5 to 90 percent.

Augite (pale tan, 2V = 45°-50°, r > v weak) or its altered equivalent occurs both as chadacrysts in plagioclase and between plagioclase grains. In the lower part of the zone the matrix pyroxene has been completely altered to green hornblende and brown biotite, but much of the chadacrystic pyroxene is unaltered. Many of the pyroxene chadacrysts are twinned, as are the amphiboles in the matrix. In the upper part of the zone, where relict pyroxene occurs in the matrix, there is a hint of a subophitic relationship in a few grains.

Opaque oxides in the lower fine-grained zone are of three types: irregular, ragged-edged to amoeboid grains with rounded silicate inclusions; anhedral to subhedral skeletal grains with vermicular, graphic, and irregular textures; and lath-shaped grains which may be partly skeletal. Interstitial quartz in this zone is intergrown with feldspar and associated with apatite.

Sill D

The lower fine-grained zone of sill D is highly porphyritic--plagioclase phenocrysts make up 30 to 60 percent of the rock (fig. 9d). They average about 5 mm in length, but some are 10 to 15 mm long. The phenocrysts are set in an intergranular matrix in which the average length of plagioclase is about 0.6 mm. The phenocrysts are subhedral to euhedral tabular grains which occur singly or as glomerocrysts; some grains are unzoned, and others show both normal and oscillatory zoning. Matrix plagioclase, which is generally more altered to sericite, occurs as very irregular equant grains, as elongate grains having rounded and scalloped edges, and as euhedral laths.

Pyroxene grains in the lower fine-grained zone are altered to green and brown hornblende and brown biotite, and original textures are obscure. Grains average about 0.3 mm in diameter. They appear to have occupied the areas between grains of plagioclase, although in the upper part of the zone a few subophitic grains were noted. Most of the pyroxene remnants either have uneven extinction, or occur as composite grains in which individuals have distinctly different optical orientations, or both.

Opaque oxides are similar to those described for the other sills. Interstitial quartz ranges from intergrowth-free anhedral grains to grains which are completely intergrown with feldspar. Apatite needles are typical associates.

Medium-Grained Zones

Medium-grained diabase (average grain size 1 to 4 mm) comprises from about 40 to 75 percent of each sill. The contacts between the medium-grained zones and the underlying fine-grained zones are gradational. Matrix plagioclase ranges in average length from 0.3 to 1.5 mm; pyroxene and its altered equivalents have average diameters between 0.4 and 1.9 mm.

The texture of the medium-grained zone of sill A is ophitic to subophitic; plagioclase occurs both in ophites of pyroxene or its altered equivalent and as clusters of several grains between ophites. Lath-shaped plagioclase grains are somewhat rounded, and ophites have irregular shapes. Several rounded grains of olivine are present in a few samples. Fe-Ti oxides include skeletal grains, lath-shaped grains, and grains having embayed margins and silicate inclusions. Interstitial quartz, typically intergrown with feldspar and associated with cluster plagioclase, is an almost invariable constituent. Alteration is variable, but typically plagioclase is partly sericitized and pyroxene grains are at least partly altered to amphibole or biotite. Modes of chemically analyzed samples are given in Table 3. A zone of slightly coarser diabase occurs between about 20 and 38 m above the base of sill A (fig. 6). The average length of plagioclase crystals in this zone is about 1.2 mm, whereas in the diabase above and below, it is about 0.6 mm. Similar zones appear to be present in the other sills, but are less pronounced.

Two subzones are recognized within the medium-grained zone of sill B. The lower subzone, extending from 1.5 to 27 m, has a subophitic to ophitic matrix and contains scattered (a few percent) plagioclase phenocrysts. It is very similar, except for the phenocrysts, to the medium-grained zone of sill A. The upper subzone, from 27 to 40 m, contains a few more phenocrysts and its matrix has an intergranular, hypidiomorphic-granular texture, although some pyroxene grains are subophitic (fig. 10a). The pyroxene in both subzones is a pale-tan augite which is partly altered to green and brown amphibole and biotite. The typical Fe-Ti oxide has embayed margins and silicate inclusions. Interstitial quartz, generally not intergrown with feldspar, is associated with clusters of plagioclase grains in both subzones. Grain sizes in the upper subzone are somewhat larger than in the lower subzone (fig. 6b). There is some indication of coarsening near the base of the lower subzone.

The original textural relations in sill C are somewhat obscure because most of the pyroxene has been replaced by green amphibole and brown biotite. However, plagioclase is enclosed or partly enclosed in amphibole grains, and so the original texture was most likely ophitic to

Table 3. Modal analyses of sill A samples for which chemical analyses are available

Sample	M11521	M11531	M11539	M11621	M11545	M11551	M11555
Height (m)	10.7	23.5	38.1	50.0	91.7	112.2	137.2
Plagioclase	45.6	47.8	47.7	44.7	43.2	42.2	47.5
Augite	20.5	17.9	17.9	14.5	19.3	9.2	3.1
Biotite	8.9	5.6	5.8	7.7	6.1	14.6	24.9
Hornblende	7.4	14.8	10.9	14.2	15.0	10.1	9.7
Opaques	7.6	4.9	7.6	7.4	7.5	4.2	4.7
Quartz	3.6	3.9	4.6	6.7	4.6	9.2	5.9
Feldspar in intergrowths	3.0	3.6	3.8	3.7	2.4	8.8	3.7
Olivine	2.1	---	0.5	---	0.3	---	---
Apatite	0.7	0.6	1.2	0.5	0.8	1.6	1.0
Calcite	0.5	---	---	0.4	---	---	---
Chlorite	0.08	0.9	0.18	0.3	---	---	---
Talc	---	---	0.09	---	1.0	---	---
Number of points counted	1187	1134	1113	1039	1022	1115	1070
Color index	47.3	44.7	44.2	44.6	50.0	39.7	43.7

subophitic (fig. 10b). Plagioclase also occurs in clusters of anhedral grains between relict ophites. The amphibole that encloses plagioclase generally has an uneven extinction and is charged with minute inclusions of opaque minerals; some amphibole grains are composite. Grains of relict pyroxene also show uneven extinction and some are composite. Minor quartz, if present, is interstitial and typically associated with plagioclase clusters. Embayed grains with silicate inclusions and skeletal grains are the most characteristic types of Fe-Ti oxides. Relative grain-size variation is shown in Figure 6b.

Plagioclase phenocrysts in an ophitic to subophitic matrix make up 5 to 10 percent of the medium-grained zone of sill D (fig. 10c). Plagioclase also occurs in clusters of several anhedral grains between ophites, although clusters are less prominent upward and are absent by the top of the zone. The pyroxene--an augite--and the Fe-Ti oxides are similar to those in other sills. Original constituents are generally obscured by alteration; alteration products compose 30 to 65 percent of the rock. Interstitial quartz is a minor constituent and in most thin sections is either not intergrown with feldspar or is involved in very simple intergrowths. Plagioclase phenocrysts are generally less than 1 cm long and matrix plagioclase is generally 1 to 2 mm long in this zone. Relative grain-size variation is shown in Figure 6c.

Plagioclase

Plagioclase occurs in three more or less distinctive settings within the medium-grained diabase. It occurs as (1) discrete, lath-shaped grains within or associated with pyroxene; (2) clusters of more anhedral grains between ophites and in association with quartz-feldspar intergrowths; and (3) phenocrysts. Grains of the first setting are elongate, and although some are euhedral, most are subhedral and have straight or embayed edges and rounded ends (fig. 11). Most of these grains are twinned according to the albite law; combined albite-Carlsbad twins are rare, and albite-pericline twins, still rarer. Most grains show normal zoning; a slightly zoned calcic inner zone comprises 50 to 85 percent of the grain, and an outer zone, the remainder. The greatest range in composition found optically was from An_{57} to An_{21}. Oscillatory zoning is rare. Sericitization ranges from minor to severe and generally does not appear to be related to compositional zones.

The plagioclase occurring as clusters between ophites is anhedral, generally more altered than in other settings, and has a more even distribution of compositional zones from core to border (fig. 12). Twinning is not as well developed in these grains. Interstitial quartz, if present, generally is associated with cluster plagioclase and may be intergrown with it along grain margins. Where associated with quartz, cluster plagioclase typically is partially altered to reddish-brown clay and sericite.

Plagioclase phenocrysts are subhedral to euhedral (fig. 10c), and occur as separate, distinct crystals and as glomerocrysts of several grains. In comparison with matrix plagioclase, phenocrysts are notably less altered, tend to be more tabular, exhibit less normal zoning (in many thin sections phenocrysts appear unzoned), have a narrower compositional range, and are slightly more calcic ($\leq An_5$). Oscillatory zoning is more evident in phenocrysts than in matrix plagioclase, and in some sections could be used to distinguish small phenocrysts from large matrix grains.

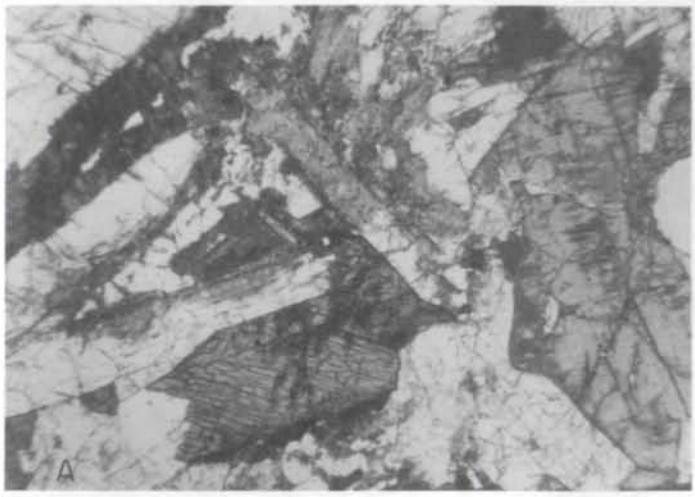

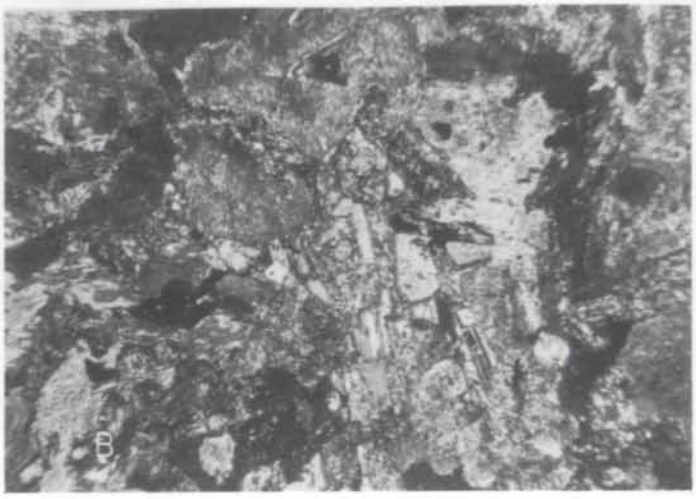

Figure 10. Textures of medium-grained zones; widths of view 3.7 mm. A, intergranular texture of the upper subzone of medium-grained zone of sill B; dark areas are pyroxene; light laths are plagioclase; some plagioclase is darkened by alteration; sample M11568, uncrossed polars. B, relict ophitic or subophitic texture of sill C; pyroxene is completely replaced by amphibole and biotite; note plagioclase laths; sample M11504, crossed polars. C, plagioclase phenocrysts in an ophitic matrix, sill D; sample M11632, crossed polars.

Figure 11. Ophitic augite. This composite ophite is made up partly of grains having slightly different optical orientations (e.g., the top part of photograph), and partly of grains having distinctly different orientations (compare top and bottom of photograph). Sample M11529; width of view 3.7 mm, crossed polars.

Figure 12. Cluster of plagioclase crystals between ophitic augite. Note that sericitization of plagioclase is more intense in the cluster. Sample M11535; width of view 3.7 mm, crossed polars.

Pyroxene

Unaltered pyroxene is colorless or pale tan, has a 2V in the range 44° to 63° (most about 52°), a weak to moderate dispersion (r > v), a lower $\underline{Z} \wedge \underline{c}$ extinction angle (40°), and is an augite. Most of the pyroxene occurs as anhedral, irregular-shaped grains in ophitic or subophitic relationship with plagioclase, although grains in the intergranular part of sill B tend to be blocky. Types of ophitic pyroxene recognized are: (1) single grains, (2) composite grains in which subgrains have slightly different optical orientations, and (3) composite grains in which subgrains have distinctly different optical orientations (fig. 11). Boundaries between subgrains in composite grains vary from straight to irregular, even between the same two subgrains. In general, however, boundaries between subgrains with markedly different orientations tend to be more regular than those between optically similar subgrains. Extinction is commonly uneven or undulatory; a more progressive extinction which suggests compositional zoning is rare. Simple {100} twins were noted in a few thin sections, but most of the pyroxene is untwinned.

No exsolution lamellae of other pyroxenes were noted. However, pigeonite was noted as small rounded grains enclosed in augite in several samples from sill A and in one from sill B.

Pyroxene is almost invariably altered to some extent and alteration ranges from minor to complete. The most common products are amphibole and biotite, but some chlorite, calcite, and opaques also are present. Alteration is commonly patchy on the scale of a thin section. Pyroxene alteration is discussed more fully at the end of the section on petrography.

Olivine

Olivine was noted in several thin sections from sills A and B, but it makes up no more than a few percent of the rock. In sill A it is most common in the interval 11 to 21 m above the base of the sill, but it also is present in thin sections from 38, 43, 87, 91, and 123 m. In sill B it occurs between 9 and 34 m.

Olivine occurs as discrete rounded grains and as rounded glomerocrysts consisting of several euhedral grains with triple point junctions (fig. 13a). Individual grains generally have diameters between 0.15 and 0.45 mm. It is common to find all of the olivine in a thin section confined to one or two parts of the section, rather than being evenly distributed.

Most of the olivine is at least partially altered. Alteration products are: (1) a mixture of talc and magnetite, (2) bowlingite, and (3) iddingsite. The most common is talc-magnetite (fig. 13b). Both minerals occur as tiny crystals, and the magnetite is typically arranged in bands within the talc; in some of these the alteration has occurred only along irregular fractures which are characterized by a concentration of opaque oxide grains. Alteration to the fibrous yellow mineral bowlingite (fig. 13c) ranges from partial to complete for a given grain; in partially altered grains bowlingite rims the olivine. Iddingsite also was identified as an olivine alteration product in several thin sections (fig. 13d). In one, some olivine grains are completely altered to iddingsite; in another, a fresh olivine core is rimmed by red iddingsite which, in turn, is rimmed by yellow bowlingite. The three types of alteration are not mutually exclusive. In sill A, for example, both bowlingite and talc-magnetite are present at 11 and 13 m, and talc-magnetite, bowlingite, and iddingsite all occur at 16 and 18 m; samples higher in the sill contain the talc-magnetite alteration, and one sample at 87 m also contains bowlingite which, although not directly associated with olivine, probably formed by alteration of olivine.

Fe-Ti Oxides

The opaque oxides are texturally the most variable and complex minerals in the diabase. Four textural types are distinguished:

Type 1. Grains having embayed margins and/or randomly distributed holes which are irregular in shape and filled with silicates (figs. 14a,b).

Type 2. Skeletal grains having a wide variety of holes which are more or less regular in shape or arrangement. These holes also contain silicates (figs. 14c,d,e).

Type 3. Lath-shaped grains (fig. 14f).

Type 4. Tiny grains of secondary opaques. All four types may be present in the same sample although one type commonly predominates. The opaques in general are closely associated with mafic silicates, and are either included or partly included in them. Average grain sizes of types 1 and 2 range from 0.2 to 0.5 mm; laths average 0.3 to 0.6 mm long.

Separates of the opaque minerals from 15 rock samples were X-rayed. All contained ilmenite but no magnetite; this was verified by cursory microprobe examination. Hematite was identified in some thin sections and its presence was indicated in a few of the X-rays.

Type 1 oxides are more common than other types in the lower parts of the medium-grained zones of sills A, B, and D, especially in the thickest sills (A and D). Grain shapes range from nearly euhedral squares and triangles in thin section (fig. 14a) to anhedral, embayed, and amoeboid grains (fig. 14b). Most grains of type 1 have irregular to rounded holes. The holes generally contain brown biotite or amphibole, but some contain pyroxene or plagioclase. Some pyroxene or plagioclase grains project into the holes from outside the oxide grain (fig. 14a). Brown or reddish-brown biotite forms a reaction rim around some opaques. Partial al-

teration to a milky leucoxene-sphene was noted in several samples.

Skeletal grains (type 2) occur throughout the medium-grained zone, but are more prevalent toward the top, except in sill C. There seems to be a complete gradation between the skeletal type and type 1. The skeletal grains display a striking variety of textures very similar to those described by Davidson and Wyllie (1968) for ilmenite in Triassic diabases in Pennsylvania. Perhaps most common is a vermicular texture where the holes are elongate, roughly parallel, and about as wide as the opaque zones between holes (fig. 14c). Also distinctive is a subgraphic texture (fig. 14d), in which the openings form patterns intermediate between typical graphic and myrmekitic textures and adjacent openings may be subparallel in part of the grain. A third type of skeletal crystal is one in which the openings appear to be crystallographically controlled. In this type, only narrow lamellae of the original opaque may remain (fig. 14e), presumably parallel to the {111} of an isometric predecessor, and the lamellae appear as discontinuous concentric sides of a triangle. In some of the skeletal grains the openings are filled with a milky-looking mixture of what appears to be sphene and leucoxene. As with type 1 opaques, holes commonly contain brown or reddish biotite and/or amphibole. In a few thin sections slight differences in reflectivity or opacity reveal that many rounded grains make up parts of some opaques.

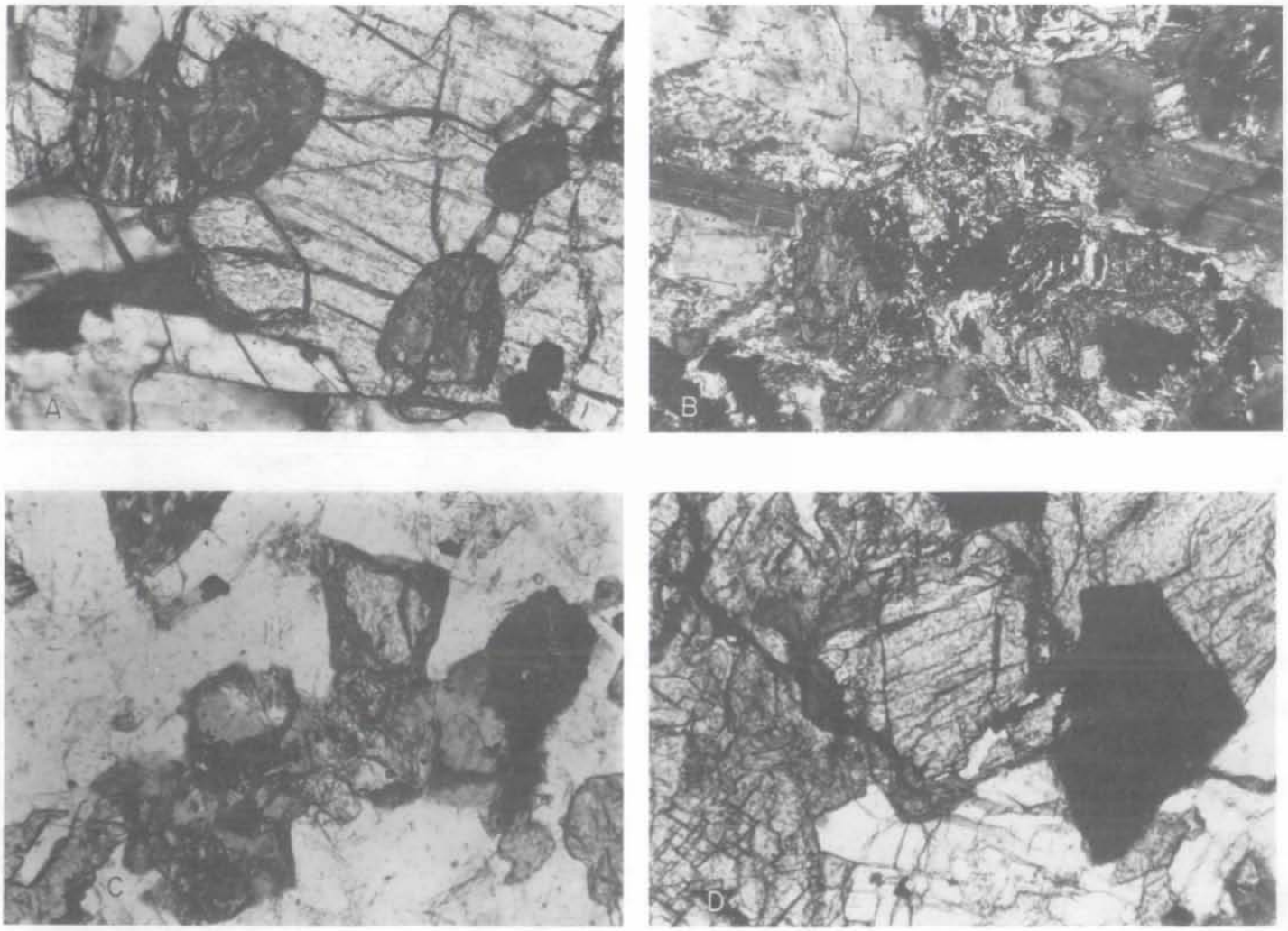

Figure 13. Olivine and alteration of olivine; width of view 0.9 mm. A, rounded grains of fairly unaltered olivine enclosed in augite; sample M11566; crossed polars. B, alteration of olivine to talc and magnetite; a few remnants of unaltered olivine; sample M11527, crossed polars. C, alteration of olivine to bowlingite; bowlingite is slightly grayer than the unaltered olivine and is to the immediate left of the opaque on the right side of the photograph and above and below the opaque in the lower center. The olivine grain left of center is unaltered on the top, but altered on the bottom. Sample M11521, uncrossed polars. D, partial rim of iddingsite (dark gray) on olivine (medium gray); sample M11566, uncrossed polars.

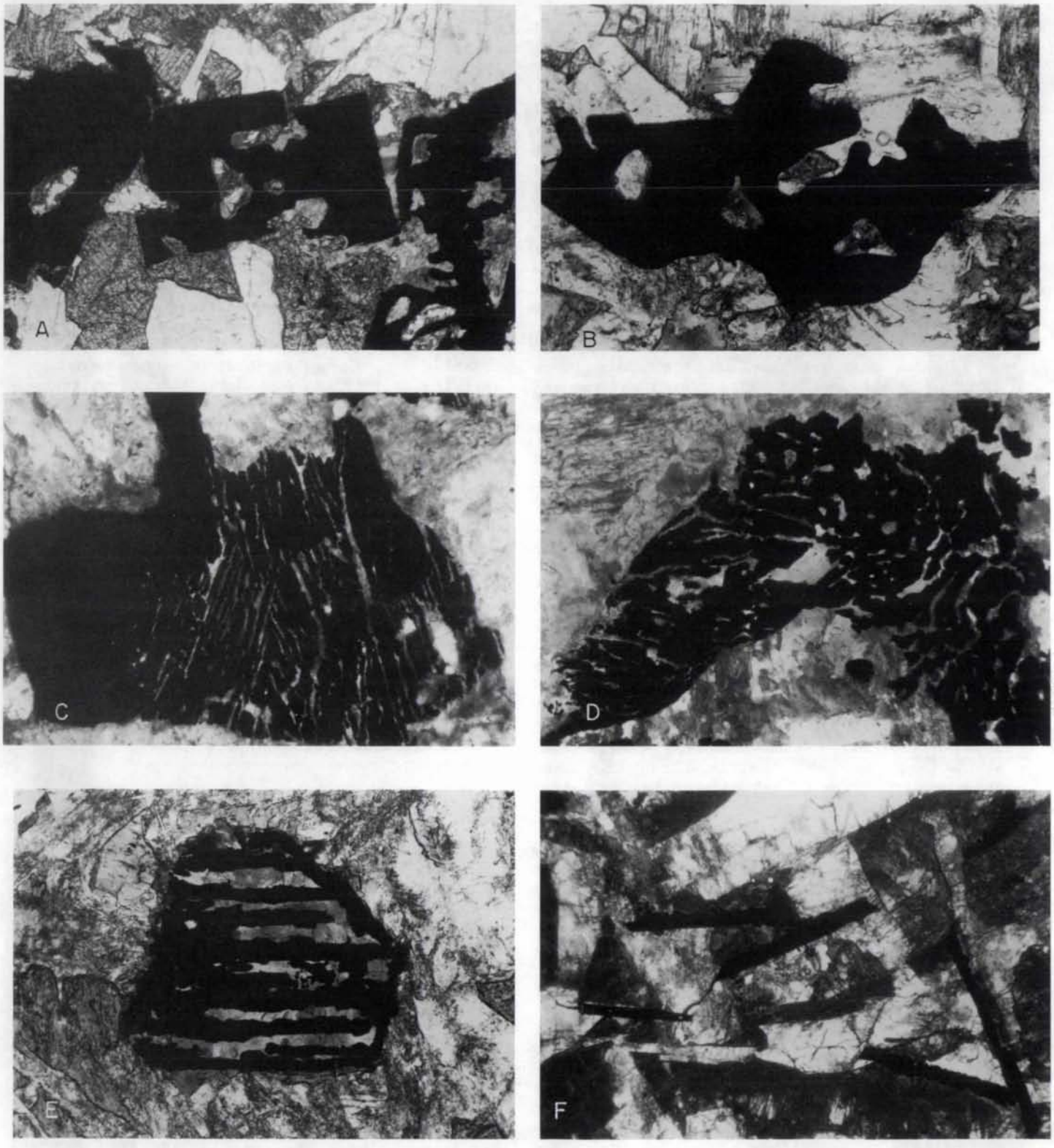

Figure 14. Textural types of ilmenite; uncrossed polars. A, grain of type 1 having isometric-like outlines which is embayed and contains holes. Note pyroxene crystal projecting into hole on top of grain; other holes contain secondary silicates. Sample M11535; width of view 2.3 mm. B, amoeboid grain of type 1; holes and embayments filled with secondary silicates. Sample M11621; width of view 0.9 mm. C, vermicular skeletal grain of type 2; note rough parallelism of holes. Sample M11555; width of view 0.9 mm. D, subgraphic skeletal grain of type 2. Sample M11552; width of view 0.7 mm. E, skeletal grain of type 2 in which lamellae seem to reflect a crystallographic control and probably parallel {111} planes of an isometric predecessor. Sample M11621; width of view 0.9 mm. F, lath-shaped grains of type 3. Sample M11623b; width of view 2.3 mm.

Type 3, lath-shaped Fe-Ti oxides are not present in all samples from the medium-grained zones. In sill A they are not present at all below 35 m, but at 56 m they are the most abundant type. In sill B they occur in the lower part of the zone but not the upper; in sill D they occur in the upper part but not the lower; and in sill C their occurrence does not seem to be related to height. In the interval from 53 to 56 m in sill A, the laths are as long as 3.8 mm, but lower in sill A and in sills B, C, and D, the laths are much smaller--less than 0.6 mm long and 0.05 mm wide. Most have slightly rounded ends and edges and are solid, but the larger ones in sill A and some in the other sills, especially sill C, are skeletal and have holes or branched edges (fig. 14f).

Oxides that are obviously secondary (type 4) occur as dustings of small ($\sim$0.01 mm) rounded grains. They are generally associated with one of the silicates formed by alteration.

Quartz and Quartz-Feldspar Intergrowths

Quartz was identified in most thin sections. It almost invariably occurs in irregularly shaped interstitial patches with average diameters of 0.2 to 0.5 mm, and is commonly associated with the plagioclase clusters described above. In many samples it is intergrown with feldspar. Intergrowths range from very simple forms, in which one or two "veinlets" of feldspar extend into an optically continuous quartz grain, to very complex micrographic intergrowths (fig. 15). The latter show a wide variety of forms including the well-known runic-character type, vermicular intergrowths, anastomosing veinlets, honeycomb, trellis, branching, and less regular forms. The feldspar in the intergrowths is almost invariably more altered than most of the plagioclase in the rock. Generally, because of the alteration, it could not be determined optically whether the feldspar is K-feldspar or plagioclase, but both were identified in a few thin sections. Most of the intergrowth feldspar appears to be in optical continuity with the adjoining zoned plagioclase, and extinction of the plagioclase passes imperceptibly into the intergrowth feldspar as the microscope stage is rotated.

Quartz includes all of the major minerals and in a few samples occurs in simple intergrowths with biotite and amphibole. Tiny needles of apatite are the most characteristic associate of quartz, and in most samples apatite occurs only as inclusions or partial inclusions in quartz.

Accessory Minerals

Apatite is the most common accessory. It occurs as small (e.g., 0.008 x 0.8 mm) interstitial needles or rods typically associated with quartz and adjoining plagioclase. Apatite is also included in amphibole in the upper part of the medium-grained zone in sill D, where two generations of it may be present. Sphene was noted in several thin sections in association with opaque minerals and presumably formed by alteration of them. In one thin section, where sphene occurs as anhedral grains up to 0.9 mm long, it is associated with sprays of slender crystals (perhaps also sphene) and a carbonate mineral (a biaxial calcite?). A few small (0.6 mm long) crystals of brookite were enclosed in amphibole in one section. Minor zircon and pyrite also are present.

Coarse-Grained Zones

A zone of coarse-grained diabase (average grain size >4 mm) comprises from 16 to 28 percent of sills A, B, and D. The contact with the underlying medium-grained diabase was not observed in the field, but was located to within 2 to 8 m. The increase in grain size (fig. 6) relative to the medium-grained zone below is striking, and if the contact is not sharp, it is gradational over a very small stratigraphic interval.

The coarse-grained zone is characterized by an intergranular allotriomorphic texture (fig. 16). Plagioclase typically occurs as randomly oriented, anhedral tabular grains. In sill B a few grains are included in pyroxene in a subophitic relationship, and there are a few plagioclase clusters. Pyroxenes (or alteration products) are anhedral, but have equant to elongate shapes. Coarse micrographic intergrowths are present in most samples. In general, both pyroxene and plagioclase are more highly altered than in all other zones except the porphyry zone; this is evident in both hand specimen and thin section. Modes of two samples from the coarse-grained zone of sill A are given in Table 3.

Plagioclase

Plagioclase grains are generally lath or tabular shaped and have irregular margins, although some are euhedral crystals. Most grains are twinned according to the albite law, but some have combined albite-Carlsbad or albite-pericline twins. In sill A, 70 to 80 percent of the grains consist of unzoned cores surrounded by narrow, normally zoned rims. In sills B and D, from half to nearly all of the individual grains show normal zoning. Plagioclase is generally sericitized, some as much as 85 percent. Sericitization does not appear to be related to compositional zoning, and is variable within individual thin sections. In sill D, irregular veinlets of red biotite cut some plagioclase grains. The same biotite also occurs with amphibole in patches which adjoin the veined plagioclase.

Pyroxene

The pyroxene, an augite, occurs as anhedral, irregular to equant to elongate grains. Most pyroxene is at least partially altered to amphibole and biotite. Both green and brown amphiboles may be present and biotite is generally brown, except in sill A where it is red. The nature of the alteration is discussed below.

Optical properties could not be determined in all thin sections, but fresh parts of grains are pale tan, have a 2V of 49° to 57°, r > v weak to moderate, and $\underline{Z} \wedge \underline{c} \sim 40°$. As in the medium-grained zones, grain types include single grains with even extinction, composite grains with slightly different extinction, and composite grains with notably different extinction; all may be present in the same thin section. A few grains are twinned. Some grains have length-to-width ratios of 4 or 5 to 1. Pyroxene grains typically include opaque minerals, and inclusions of apatite and plagioclase were also noted in a few samples.

Fe-Ti Oxides

All four types of oxides occur in the coarse-grained zones, but type 2 skeletal grains are the most prominent. Of these, most are vermicular; subgraphic and irregular types also are common, but lamellar crystallographically controlled types are rare. Grains of types 1 and 2 average 0.3 to 0.9 mm, but grains as large as 1.6 mm occur.

In sill D, grains of type 1 are nearly as abundant as type 2 grains, but many of the type 1 grains are partly skeletal. Type 1 grains are euhedral to anhedral, but generally are embayed and contain silicate inclusions.

Parts of many of the type 1 and type 2 grains are altered to milky leucoxene-sphene ± brown or red biotite. Some tiny (<0.01 mm) rounded opaque oxide remnants occur within the milky alteration product. Hematite is a common associate in sill A.

Lath-shaped (type 3) oxides are not abundant in the coarse-grained diabase, and where present are typically skeletal. Average lath lengths are 0.7 to 1.5 mm and the maximum is 5.6 mm. Lath margins are generally rounded, but are straight in a few samples.

Secondary oxides (type 4) mostly occur as small rounded "dusty" grains. In one sample from sill A, however, an elongate grain of pyroxene contains subhedral to anhedral grains of opaques which are associated with a central "rib" of red hematite. The opaques in this grain are generally elongate perpendicular to the rib; most are strongly embayed, but some have subhedral outlines.

Quartz and Quartz-Feldspar Intergrowths

Quartz occurs both as separate grains and intergrown with feldspar, and is invariably interstitial. Separate grains are anhedral, irregularly shaped, and have diameters as large as 1.2 mm. Quartz-feldspar intergrowths are generally larger and coarser than in other zones. A wide variety of intergrowth patterns includes runic, anastomosing, branching, radiating, and vermicular forms, as well as simple forms. In general, intergrowths are with adjoining plagioclase grains, and extinction of the plagioclase passes from the plagioclase core into the intergrowth feldspar without interruption. In several samples the contact between adjacent plagioclase grains occurs within the intergrowth. Plagioclase adjacent to quartz is typically altered to a reddish-brown kaolin and sericite, as in the medium-grained zone.

Apatite needles are almost invariably associated with quartz, and calcite is associated with quartz in a few sections. Quartz includes all other minerals.

Accessory Minerals

Apatite is present in all thin sections, generally in association with quartz. Its crystals are larger than in the underlying zones; one was as large as 1.8 x 0.05 mm. Apatite crystals included in plagioclase and amphibole or pyroxene tend to be larger than those in quartz. There may be two generations of apatite.

Other accessory minerals include pyrite, which was noted in only a few sections, and zircon included in amphibole and biotite. Olivine was noted in only one thin section from sill B and only one grain was seen.

Upper Medium-Grained Zones

A medium-grained diabase separates the coarse-grained zone below from the porphyritic zone above in sills A and B, and possibly in sill D as well, although no exposures were found. The contact between the medium-grained diabase and the underlying coarse-grained diabase appears to be gradational, whereas the contact with the porphyry is sharp. The medium-grained diabase has a subophitic to intergranular texture, and contains scattered plagioclase phenocrysts near the top of the zone in sill B. Matrix plagioclase averages 1.5 mm long, and most augite grains have diameters of 0.7 to 1.8 mm.

Plagioclase occurs as randomly distributed grains, as well as clusters of grains. It is twinned and normally zoned. Most grains are lath-shaped, although margins are typically rounded or embayed. The pyroxene has a 2V ∿51° and is an augite. It occurs as single grains and as composite grains in which individual members have notably different optical orientations. Most of the pyroxene is partly altered to amphibole or biotite. Types 1, 2, and 3 Fe-Ti oxides are present, but most are type 1, equant to elongate, embayed grains. Quartz is interstitial and some is intergrown with feldspar.

Porphyry or Porphyritic Zones

A porphyritic zone occurs in the upper parts of all four sills, comprising 3 to 23 percent of the sills (fig. 5). In sills A and B, plagioclase phenocrysts averaging 10 to 25 mm long make up 50 to 60 percent of the rock (fig. 17a). In sill C phenocrysts averaging 5 to 15 mm in length make up only a few percent of the rock. In sill D the phenocrysts are only ∿5 to

10 mm long, approximately the average grain size of the underlying coarse-grained zone; they make up 10 to 70 percent of the rock. The matrix in all sills is medium grained.

The contact between the porphyry and underlying medium-grained zone was observed only in sills A and B. In sill A it is marked by the abrupt appearance of phenocrysts in a matrix which appears identical with the underlying rock. In sill B the contact is similar, but scattered phenocrysts also occur in the underlying medium-grained diabase. In neither sill does the contact appear to be intrusive, but is defined by crystal faces and thus is irregular in detail. The upper contact was observed only in sill B. It is much like the lower contact in that scattered phenocrysts, identical to those in the porphyry, occur in the overlying diabase; the matrix of the overlying diabase, however, is finer grained than that of the porphyry.

The texture of the matrix is variable. In sill C, where there are few phenocrysts, the matrix has an ophitic to subophitic texture; plagioclase laths average 1.9 mm in length, and ophites or remnant ophites average about 2.7 mm in diameter. In sill B the matrix is so altered that the original texture is difficult to discern, but it appears to be intergranular (fig. 17b). Matrix plagioclase in sill B has average lengths of 1 to 2 mm, whereas the amphibole, presumably derived from pyroxene, has average diameters of 0.3 to 0.8 mm. In sill D the matrix is ophitic to subophitic, even in samples containing as much as 70 percent phenocrysts.

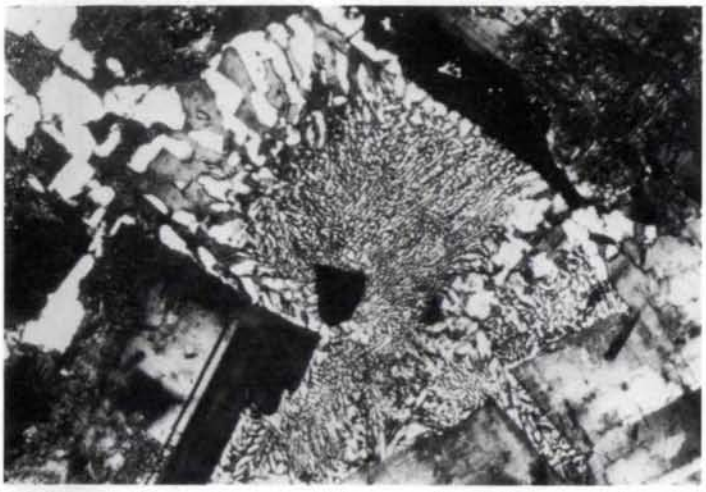

Figure 15. Micrographic quartz-feldspar intergrowths. Note variation in size and texture of intergrowths. Sample M11554; width of view 2.3 mm, crossed polars.

Figure 16. Intergranular texture in a coarse-grained zone. Textured gray mineral at center and bottom is partially altered pyroxene. Note micrographic intergrowths. Sample M11571; width of view 3.7 mm, crossed polars.

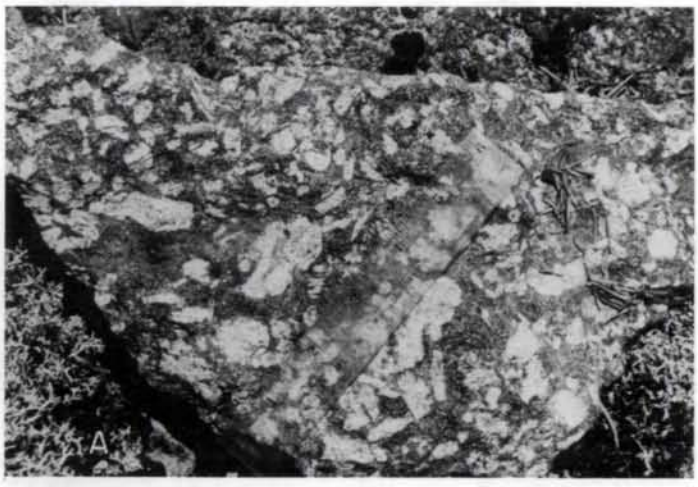

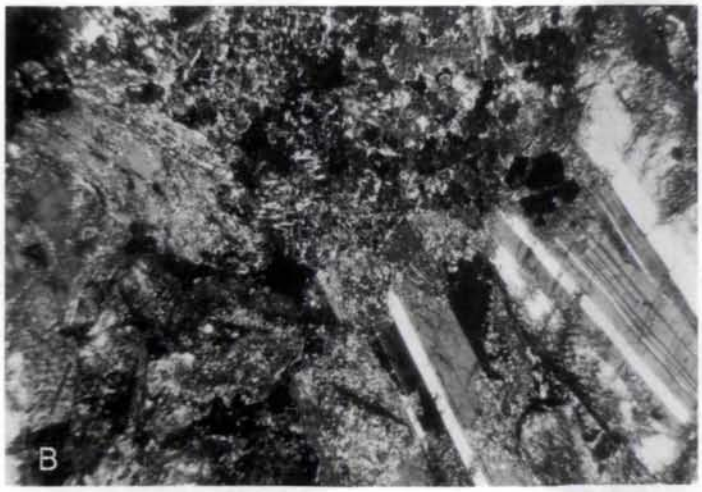

Figure 17. Porphyry zone. A, block of porphyry from near the top of sill A, southwest of Mucker Lake; white phenocrysts are plagioclase. B, plagioclase phenocryst (right) set in an altered intergranular(?) matrix. Sample M11576; width of photomicrograph 9.2 mm, crossed polars.

Matrix plagioclase in sill D has average long dimensions of 0.4 to 0.6 mm, and pyroxene or altered equivalent has average diameters in the range 1.5 to 2.1 mm. All samples having ophitic or subophitic textures also contain clusters of plagioclase grains, generally associated with quartz-feldspar intergrowths.

Plagioclase

Plagioclase phenocrysts are generally tabular, but grain shapes vary from long, narrow laths to equant. Most grains are anhedral with rounded and irregular margins, but a few are subhedral, generally with straight sides and irregular ends. Shapes of matrix plagioclase grains are generally similar to phyric grains in variety, but on average are more irregular. Both matrix and phyric plagioclase are twinned; albite twins are prevalent; albite-Carlsbad and albite-pericline twins are rare. Strong normal zoning is evident in matrix plagioclase. Phenocrysts show only minor normal zoning, but oscillatory zoning is evident in many crystals. Matrix plagioclase is noticeably more altered than phyric plagioclase in most samples. Alteration is generally to sericite, although in sill B calcite and chlorite also appear to have formed, in part, by alteration of plagioclase. Phenocrysts generally do not include other minerals. The matrix plagioclase in sill B, however, is poikilitic, containing small rounded grains of amphibole and Fe-Ti oxides.

Pyroxene

Most of the pyroxene within the porphyry zones has been altered to amphibole-biotite, and in sill B no pyroxene remains. The pyroxene in sills C and D is pale tan, has a 2V $\sim$ 51°, is confined to the matrix, and typically occurs as small rounded remnants within amphibole-biotite. It is an augite similar to the pyroxene in lower zones. In sills C and D, where the matrix is ophitic, grain shapes are inferred to be irregular, and ophites or relict ophites appear to include single, optically continuous grains, composite grains with similar optical orientations, and composite grains with different optical orientations. Pyroxene (or altered equivalent) includes opaque minerals and, if ophitic, plagioclase.

In sill B pyroxene is altered to brown and green amphibole, chlorite, and in one thin section, red biotite. In sill C green to olive amphibole, reddish-brown biotite, and minor green biotite are the alteration products, and in sill D green amphibole and reddish-brown biotite are typical. Pyroxene alteration is further discussed below.

Fe-Ti Oxides

The nature of the oxides in the porphyry zone is somewhat variable from sill to sill, although the three primary textural types are present in all sills. In sill B relative abundances vary within the zone, and relative percentages are difficult to determine in the lower part where all types are partly altered to a brownish, milky leucoxene-sphene mixture. Skeletal (type 2) grains have irregular, vermicular, subgraphic, and crystallographically controlled textures. Type 2 grains predominate near the center of the porphyry zone of sill B, and type 3 grains, in the upper part. Typical type 3 grains occur in groups of two or three parallel laths; some laths consist of lines of triangular grains, and many laths are partly skeletal and have frayed margins. Some of the skeletal laths in the upper part of sill B have vermicular holes that are normal to the long dimension of the lath and look like short branches.

Quartz and Quartz-Feldspar Intergrowths

Quartz is invariably interstitial in the porphyry zone and is generally intergrown with feldspar. Intergrowths vary from simple to complex, but most are irregular "veinlets" of feldspar in quartz, and many are confined to edges of quartz grains. As in other zones, the extinction of adjoining zoned plagioclase passes outward from the plagioclase core into the intergrowth feldspar. Apatite needles are an almost invariable associate of quartz.

Accessory Minerals

Apatite occurs in association with quartz in all sections examined. It also is included in plagioclase and amphibole in one sample from sill D. Some zircon surrounded by pleochroic halos occurs in amphibole.

Upper Fine-Grained Zones

The upper fine-grained zones, which comprise 2 to 13 percent of the sills, are similar in many respects to the lower fine-grained zones. The upper fine-grained zone of sill A was not observed in the field; its presence is inferred and its thickness is estimated by comparison with the other sills and probable sill thickness. The thickness of the zone in sill B, where faulting has occurred, also is estimated.

All of the observed upper fine-grained zones have an intergranular texture, and all are somewhat porphyritic, at least in part. Average lengths of matrix plagioclase laths in this zone are 0.2 to 0.9 mm, decreasing in size as the upper chilled margin is approached. Phenocrysts are 3 to 16 mm long in sill B, but only 1 to 5 mm in sills C and D. No pyroxene was identified in this zone in any of the sills; it apparently has been replaced by amphibole and biotite, and in one thin section, by chlorite. The average diameter of amphibole grains is 0.2 to 0.6 mm. Interstitial quartz is present in all samples, but in sill B rounded polycrystalline aggregates of quartz, 1 to 1.8 mm in diameter, occur as well. These aggregates may be xenoliths of the overlying Rove Formation; however, they include, in addition to plagioclase, Fe-Ti oxides with textures identical to the opaques in the surrounding diabase.

The matrix in the upper fine-grained zone is generally quite altered--half to nearly all of the primary minerals are gone. Matrix plagioclase grains range in shape from laths with rounded or irregular margins to irregular. They are albite twinned and normally zoned. Sericitization is variable and patchy within any given thin section. The amphibole, probably a hornblende, is generally pale green to green (some brown amphibole occurs in sill B), has $\underline{Z} \wedge \underline{c}$ = 16° to 21°, and occurs as irregularly shaped equant to elongate grains. Grains typically show an uneven extinction and contain tiny inclusions of opaque minerals or biotite or both.

Fe-Ti oxides are chiefly of types 1 and 3, especially toward the top of the zone. Type 1 oxides typically are irregularly shaped with embayed margins, have average diameters of 0.06 to 0.15 mm, and may or may not have holes. In sill B they occur in aggregates of small (0.02 to 0.08 mm), ragged-edged, round grains; aggregate diameters are 0.1 to 0.3 mm. Type 3 laths are variable--margins are straight, ragged, or branching, and some laths are partly skeletal; lengths range from 0.2 to 0.9 mm. They are randomly distributed or occur in groups of parallel laths. Skeletal oxides (type 2) are present in sill C and in the base of the zone in sill B.

Interstitial quartz and associated apatite needles are present in all samples. In general, quartz is not intergrown with feldspar, although some simple intergrowths were observed.

Upper Chilled Margins

The upper chilled margins of sills B, C, and D are exposed (fig. 18a), and are very similar to the lower chilled margins of these sills. The upper chilled margins are 0.3 to 0.6 m thick, very fine grained, and contain sparsely scattered plagioclase phenocrysts set in a felty, intergranular matrix, except for sill D where phenocrysts make up 5 to 10 percent of the chilled margin. The matrices are composed of poorly defined to lath-shaped plagioclase, pale-green or brown, irregular to elongate amphibole, brown to red biotite, granular to acicular Fe-Ti oxides, and interstitial quartz. Brown to red-brown biotite, rather than amphibole, occurs within <1 to 3 cm of the contact in sills B and D. In sill D it occurs both as small (<0.08 mm) ragged grains and as larger (0.1 to 0.2 mm) poikilitic grains containing Fe-Ti oxides and feldspar.

Inclusions

The upper chilled margins of sills C and D contain xenoliths of Rove Formation quartzite (fig. 18b) and autoliths of anorthositic diabase porphyry (fig. 18c); both range in diameter from 2 to 45 cm. The autoliths in sill C contain labradorite phenocrysts set in a matrix of fine-grained diabase like the surrounding rock, and hence the presumption that they are autoliths rather than xenoliths. These phenocrysts are so abundant that they touch each other; they are unzoned, tabular but anhedral, and sericitized. The autoliths in sill D are similar, but the phenocrysts they contain are larger, some as long as 2 cm.

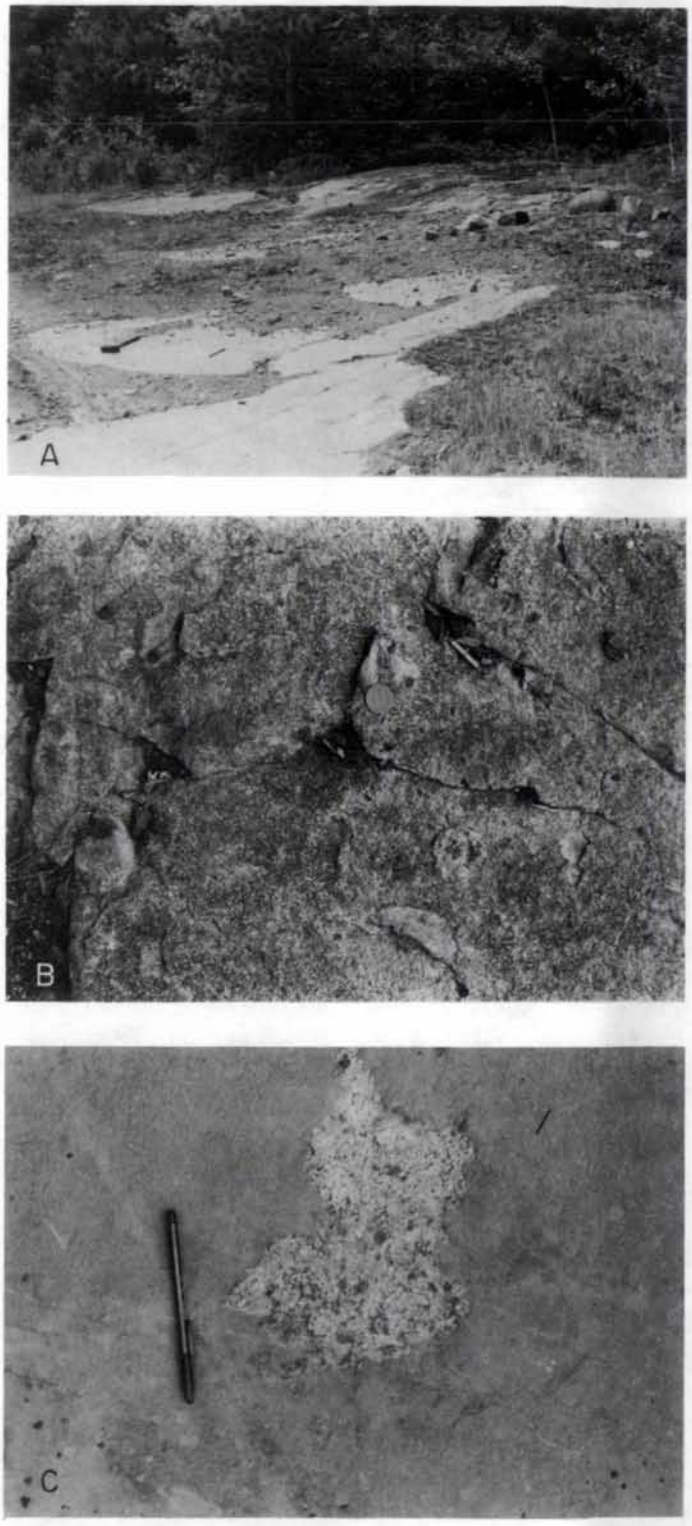

Figure 18. Upper chilled margin. A, gently dipping chilled top of sill C. B, xenoliths of Rove Formation quartzite in the top of sill C; penny near center is on the edge of one xenolith and another xenolith is near bottom center. C, autolith of anorthositic diabase porphyry, top of sill C.

Pyroxene Alteration

Pyroxene in thin sections from all zones is at least partly altered. In general, the degree of alteration is variable on the scale of a thin section; in some thin sections, alteration is more intense near interstitial quartz-feldspar intergrowths. The most typical alteration products are green and brown varieties of amphibole (hornblende) and biotite, but opaque oxides are common and chlorite was noted in some samples. Textural types of alteration are (1) marginal, (2) pervasive or cleavage-related, and (3) patch. One or all of these types may be present in a given sample.

Marginal Alteration

In thin sections containing pyroxene, the rims of at least some of the pyroxene grains have been altered to amphibole or biotite (fig. 19a). The alteration is variable in texture and somewhat variable in mineralogy. Most typical, perhaps, is a whole or partial rim of optically continuous green or, less commonly, brown hornblende. The optically continuous hornblende commonly contains inclusions of (1) somewhat rounded, small (0.01 to 0.05 mm) grains of hornblende with different optical orientations, (2) similar-sized, somewhat rounded grains of brown biotite, or (3) tiny (0.002 to 0.008 mm) grains of an opaque mineral. Individual grains may contain one or all of these types of inclusions, but in any thin section one type generally predominates, even to the near exclusion of the others. In rare single grains, part contains inclusions and part is inclusion-free.

Just as some pyroxene ophites are composites of grains which have similar or different optical orientations, some amphibole rims are composites of grains which have similar or different optical orientations. These rims are typically green, but some are brown; they may contain or be free of the types of inclusions described above.

The smaller the individual crystal rimmed by composite-grain hornblende, the more the rim resembles the patch type of alteration described below, and the rim then consists of small (0.04 to 0.15 mm) grains of amphibole and/or biotite. This type of rim is less common than other types.

Combinations of rim types were observed. In a few thin sections the pyroxene is directly rimmed by a patch-type green amphibole containing many tiny opaque inclusions; the patch-type amphibole is in turn rimmed by an optically continuous green hornblende with or without inclusions. The reverse, i.e., optically continuous rimmed by patch type, also occurs. Another combination observed in a few samples is an optically continuous hornblende grain containing inclusions of patches. One rim consists of the following sequence: pyroxene - optically continuous brown hornblende - optically continuous green hornblende - optically continuous green biotite - patch-type green amphibole.

The mineralogy of the altered rims is variable. By far the most common mineral is a green hornblende. In a few samples two shades of green on the same optically continuous rim suggest chemical zoning. In one sample some rims are very pale green adjacent to the pyroxene and darker green farther away, but other rims are olive green adjacent to the pyroxene and lighter green farther away, and some grains show no color zoning.

Brown hornblende, although less common, is present in many samples. Some hornblende rims around a pyroxene are entirely brown, and some are part brown and part green. Where both brown and green hornblende compose the rim, they extinguish simultaneously and are obviously crystallographically continuous. Most commonly the brown hornblende is adjacent to the pyroxene and green hornblende rims the brown, but the opposite also occurs.

Biotite makes up all or part of the altered rims in many samples. Brown biotite is more common, but green biotite occurs along with the brown in some samples. In some samples biotite occurs as small grains within the amphibole, but more commonly it forms a distinct part of the marginal zone. A typical sequence is pyroxene - hornblende - biotite, but the sequence pyroxene - biotite - hornblende was observed, as well as pyroxene grains rimmed in part by hornblende and in part by biotite. All three of these combinations were observed in a few samples. Biotite rims occur as single, optically continuous grains and also as composites of grains having different optical orientations. Some of the latter consist of both green and brown biotite.

Pervasive or Cleavage-Related Alteration

In many samples, especially from the coarse-grained zones, parts of the pyroxene grains appear to be charged with tiny ($\leq$0.005 mm, fig. 19b) grains, which presumably are incipient crystals of amphibole and/or biotite. They appear gray, grayish brown, tan, brown, dark brown, or reddish brown, and are readily distinguished in plane-polarized light. Some of these altered areas are parallel linear bands in two dimensions, and are apparently related to cleavage. The pervasive type of alteration, where large areas of a pyroxene grain are altered, bears no apparent relation to crystallographic directions. In most samples both cleavage and pervasive types of alteration are more prevalent around grain rims, but in a few samples the distribution is random. It is not uncommon to see a clean pyroxene core, a pervasively altered zone, and a rim of any of the marginal alteration types. In a few samples the pyroxene has been completely replaced by an optically continuous hornblende, yet the amphibole contains a core or several areas containing pervasive-type alteration products. One would expect that, had reaction proceeded a little further, the pervasive-type material would have been assimilated within the optically continuous hornblende.

A variant of pervasive alteration is one in which pyroxene contains scattered and larger (0.01 to 0.05 mm) grains of amphibole or biotite. Such grains are easily identified, widely separated, and show no preferred distribution.

Patch Alteration

A very distinctive type of pyroxene alteration in these diabases is one in which patches of small grains of amphibole, biotite, chlorite, or mixtures of these minerals occur apart from any pyroxene (figs. 19c, d). The patches have diameters of 0.3 to 3 mm and an allotriomorphic-granular texture. Grain size ranges from 0.01 to 0.15 mm; most prevalent are the ranges 0.02 to 0.04 mm, and 0.08 to 0.12 mm. Most patches contain grains of either one size range or the other, although some patches in many samples consist of a cluster of larger grains surrounded by smaller grains.

Individual grains in a patch typically are equant but anhedral, and have indistinct margins and uneven or wavy extinction. In some patches amphibole grains are fibrous; in others, grains of biotite, amphibole, or chlorite occur as shredlike grains with frayed ends.

The amphibole in most patches is green, but some brown amphibole, which tends to be slightly larger than the green variety, also occurs. Both brown and green biotite occur; in sill A most patches consist of green biotite, but in the other sills brown is more common. Most patches contain mixtures of green hornblende and brown

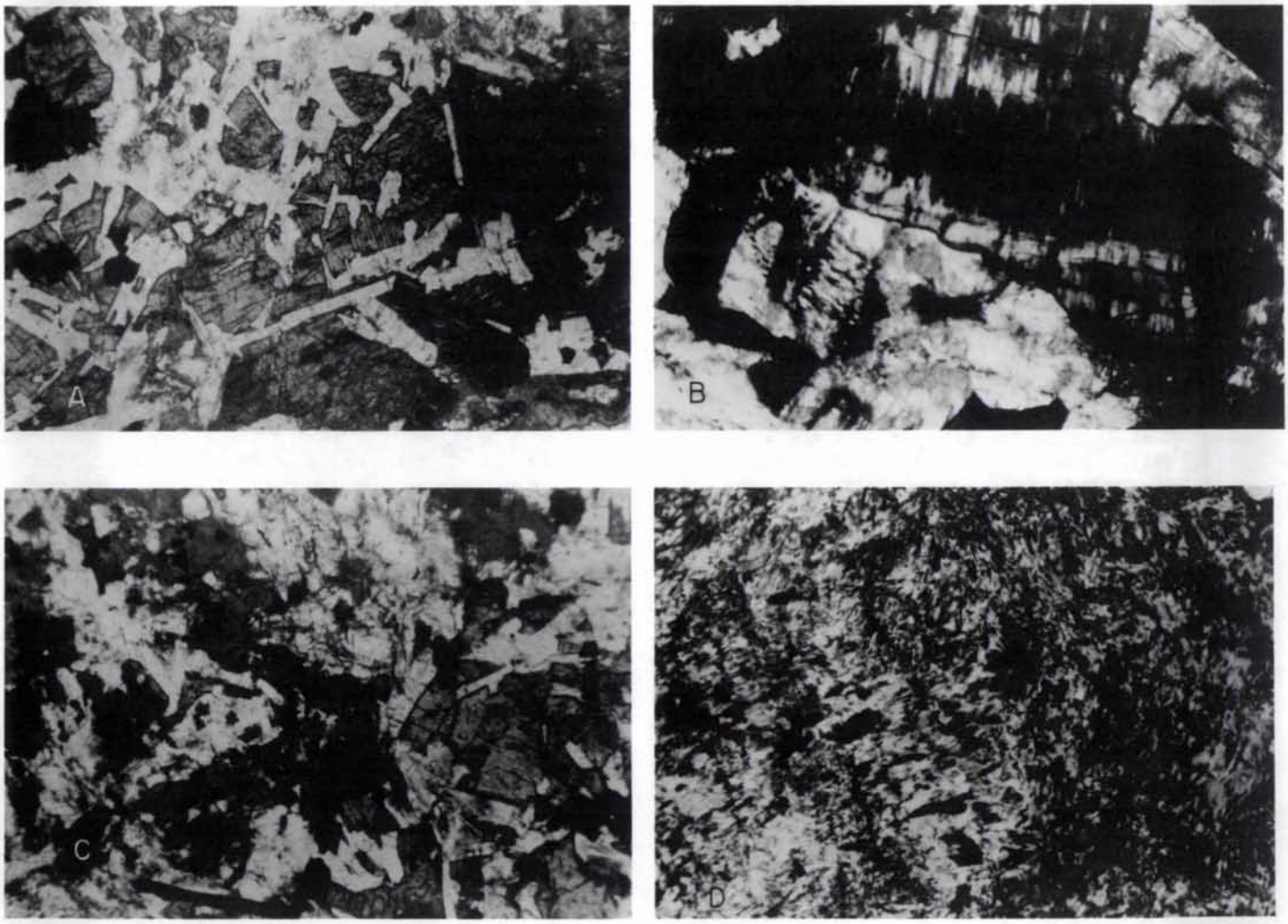

Figure 19. Pyroxene alteration. A, marginal alteration. Augite ophite (gray) has partial rim of brown hornblende (darker gray, right side of photomicrograph). Note cleavage in hornblende. Sample M11521; width of view 3.7 mm, uncrossed polars. B, cleavage-related alteration. Tiny grains of brown hornblende or biotite in center of pyroxene extend outward along preferred planes. Sample M11554; width of view 3.7 mm, uncrossed polars. C, patch alteration. Fuzzy-looking area is patch of amphibole-biotite derived from alteration of pyroxene. Note unaltered pyroxene on right. Sample M11519; width of view 2.3 mm, crossed polars. D, patch alteration. Mat of fibrous amphibole derived from patch-type alteration of pyroxene. Sample M11627; width of view 0.9 mm, crossed polars.

biotite, but some are monomineralic. Patches of chlorite are much less abundant than patches of either biotite or hornblende. In some samples a reddish or reddish-brown biotite occurs and calcite was noted in a few samples. Some patches contain tiny grains of opaque minerals.

No relationship between patches and pyroxene is evident in many samples. However, patch-type alteration products rimming some pyroxene grains suggest that it is safe to attribute the patches to alteration of pyroxene.

Relation to Sill Stratigraphy

Only a few generalizations can be made about pyroxene alteration relative to sill stratigraphy. The chilled margins and fine-grained zones contain little or no pyroxene. Where pyroxene is present in these zones, alteration is only of the marginal type.

In the medium-grained zones, all described types of pyroxene alteration occur, but relative abundances are variable, not only from sill to sill, but from sample to sample. There does seem to be some relationship to fabric. The pervasive type of alteration is generally minor or absent in medium-grained ophitic zones, but it is prominent in the medium-grained intergranular zone of sill B. Marginal and patch alteration are about equally abundant in the medium-grained zones. In sills A and B, brown and green amphibole and brown and green biotite are alteration products, whereas in sills C and D, green amphibole, minor brown amphibole, and brown biotite were formed.

Coarse-grained zones are characterized by pervasive alteration, and in sills A and D, by reddish biotite. Marginal and patch alteration to brown and green amphibole also occur in this zone.

The porphyry zones contain little pyroxene; most has been altered to green amphibole and brown biotite or chlorite. The little pyroxene remaining shows all three types of alteration.

In a few thin sections from the medium-grained ophitic to subophitic zone of sill A, euhedral crystals of biotite or amphibole may be primary rather than secondary minerals. These grains are not associated with pyroxene or with obviously secondary biotite or amphibole. They have roughly the same grain size as the plagioclase in the same rock.

ROCK CHEMISTRY

Fifteen new whole-rock analyses for major oxides are presented in Table A-1 along with their CIPW norms; corresponding modes for the medium- and coarse-grained zones from sill A are given in Table 3. In comparison to average dolerite, diabase, basalt, and tholeiite (Le Maitre, 1976), the sills have low values for Al_2O_3, CaO, and MgO and high values for Fe, K_2O, P_2O_5, and especially TiO_2. In general Al_2O_3 <14, CaO <8, MgO <5, and Fe as FeO >13, K_2O >1, P_2O_5 >0.3, and TiO_2 >3 weight percent. Geul (1970), Weiblen and others (1972), Mudrey (1973), and Weiblen and Morey (1975) have noted these characteristics in other Logan intrusions. All but two samples are Q-normative.

Because the sills very likely were formed during an episode of rifting (e.g., Chase and Gilmer, 1973), it is also of interest to compare them with mid-ocean ridge basalts (MORB) (fig. 20). Al_2O_3, MgO, MnO, and CaO are lower in the sills than in MORB, but total iron as FeO, Na_2O, K_2O, TiO_2, P_2O_5, and loss on ignition (= H_2O^+ + H_2O^- + CO_2 for sills) are higher. The high values for K_2O, TiO_2, and P_2O_5 are particularly striking, as is the similarity of sills A and B.

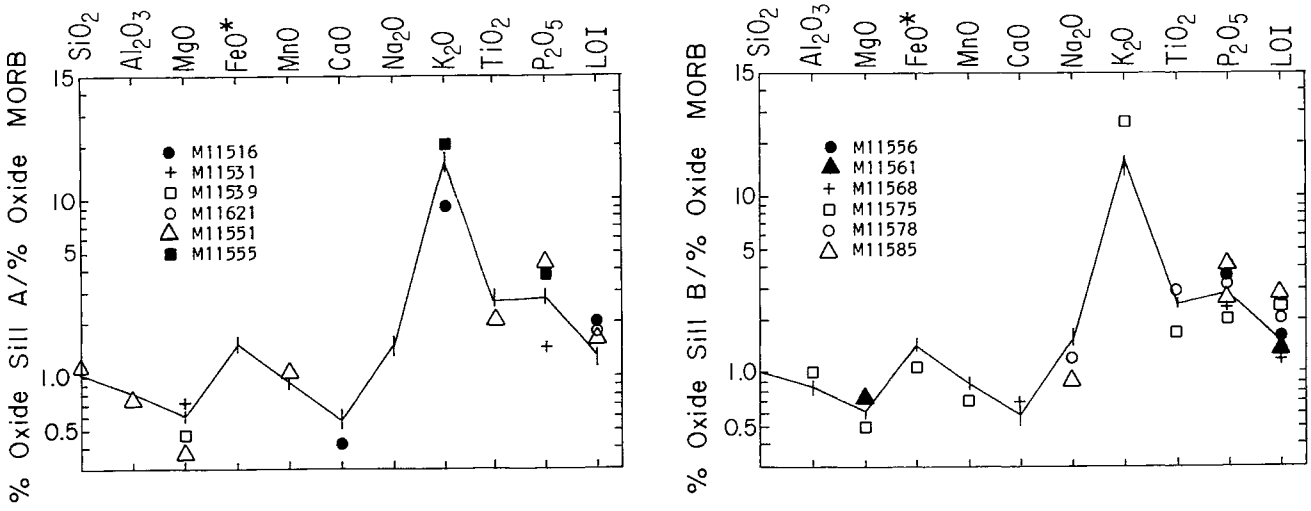

Figure 20. Comparison of major-element chemistry of sill A (left) and sill B (right) with an average value for Cretaceous MORB (MORB data from Jahn and others, 1980). Lines connect points representing whole sill values. Vertical bars show range of closely spaced values; points outside this range are indicated by symbols representing specific samples. FeO*, total iron as FeO; LOI, loss on ignition.

Included in Table A-1 are whole-sill bulk analyses of sills A and B calculated using the stratigraphic data in Figure 5 and the analyses of individual samples. The bulk composition of sill A was obtained by assuming that 76 percent of the sill (the fine- and medium-grained zones) could be represented by the average of the analyses for M11521, M11531, M11539, M11621, and M11545; that 21 percent of the sill (the coarse-grained zone) could be represented by the average of analyses for M11551 and M11555; and that the remaining 3.1 percent (the porphyry zone) could be represented by M11575 (from sill B). The bulk composition of sill B was obtained from 15.6 percent of M11578 (representing upper and lower fine-grained zones), 32.5 percent of M11561 (representing the medium-grained ophitic zone), 22.1 percent from M11568 (the medium-grained intergranular zones), 15.6 percent from the average of M11551 and M11555 (coarse-grained zone), and 14.3 percent from M11575 (the porphyry). Comparison of whole-sill analyses with chilled margins (M11516 for sill A; M11556 and M11585 for sill B) suggests that the chilled margin does not fairly represent the bulk chemistry of the sills. On average, the whole sills appear to be depleted in SiO_2, TiO_2, Fe, and P_2O_5 and enriched in Al_2O_3, CaO, MgO, Na_2O, and K_2O relative to the chilled margins.

The mineralogy of the sills indicates that they are tholeiites, but classification in terms of chemistry, using the criteria of Irvine and Baragar (1971), is less clear. Samples plotted on a SiO_2 vs Na_2O-K_2O diagram (fig. 21) fall on both sides of the dividing line between alkaline and subalkaline rock. However, when the same data are plotted on the Irvine-Baragar Ol'-Ne'-Q' diagram (fig. 22), all but one sample are subalkaline. If all samples are treated as subalkaline, they are clearly tholeiitic rather than calc-alkaline, again using the Irvine-Baragar criteria. Most samples have "average" K contents (fig. 23) and are "basalts" (fig. 24) in the Irvine-Baragar classification.

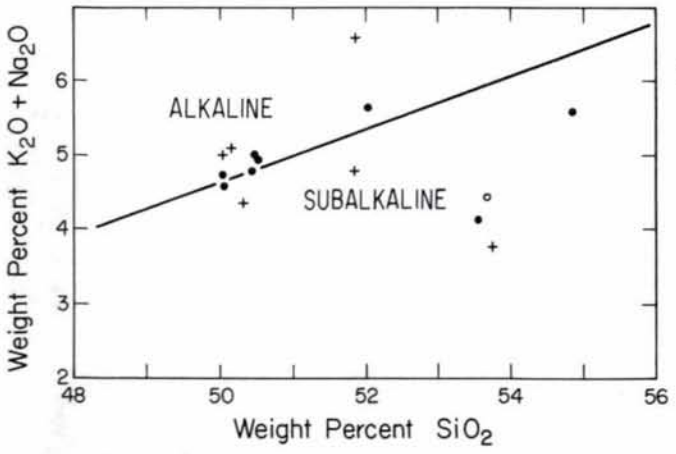

Figure 21. Alkali-silica plot of data adjusted for alteration using method of Irvine and Baragar (1971); •, sill A; +, sill B; o, sill D.

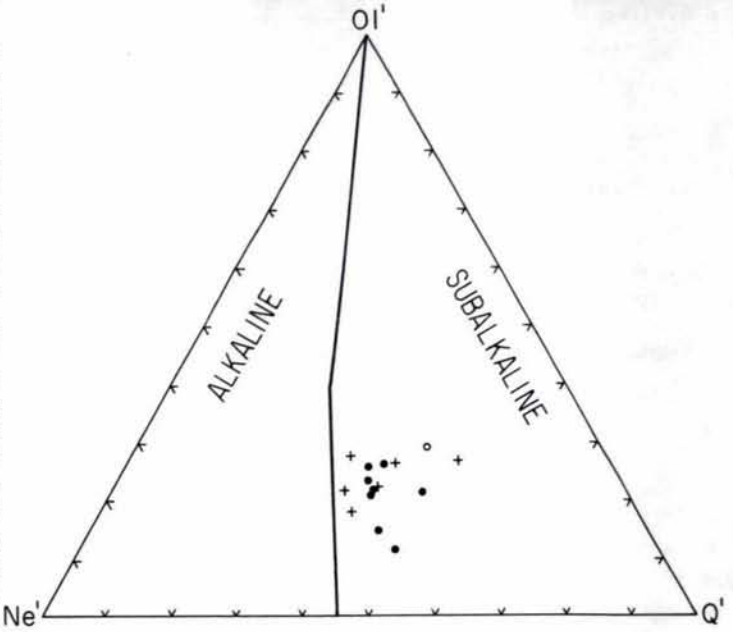

Figure 22. Plot of Ne' (= Ne + Ab) - Q' (= Q + 2/5 Ab + 1/4 Opx) - Ol' (= Ol + 3/4 Opx) where Ne, Ab, Q, Opx, and Ol are cation norm minerals (after Irvine and Baragar, 1971); •, sill A; +, sill B; o, sill D.

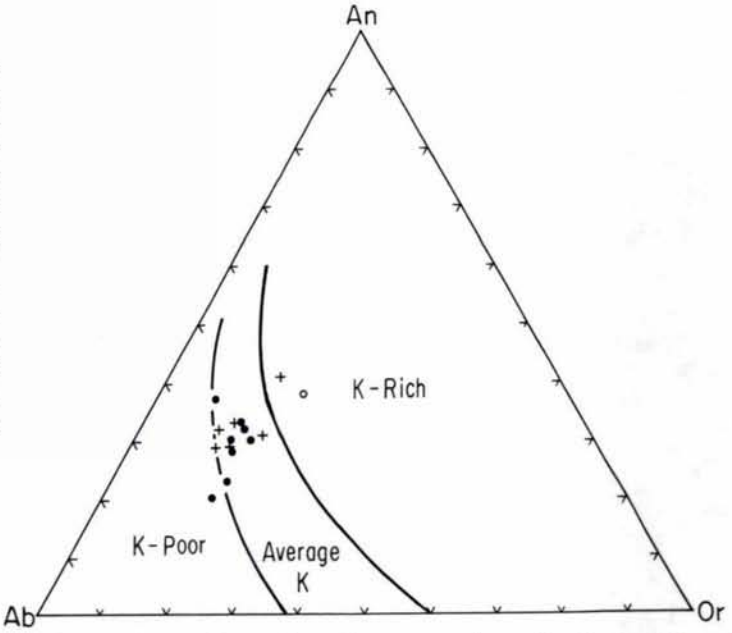

Figure 23. Plot of cation norm minerals Ab-An-Or (after Irvine and Baragar, 1971); •, sill A; +, sill B; o, sill D. Most samples have average K contents. The one K-poor sample is from the coarse-grained zone of sill A; the K-rich sample from sill B is from the upper chilled margin.

Major oxides are plotted against SiO_2 and MgO in Figure 25. There is a surprising amount of scatter considering the close relationship between these rocks. The only well-defined trends are (1) decrease in MgO, CaO, and, though less well defined, TiO_2 with increase in SiO_2; and (2) increase in P_2O_5 and, though poorly defined, K_2O with increase in SiO_2. FeO, Fe_2O_3, total Fe, Al_2O_3, and K_2O vary irregularly or almost not at all with change in SiO_2. The one analysis from a porphyry zone, in particular, shows marked deviations in the trends for iron, Al_2O_3, CaO, K_2O, and TiO_2. Weiblen and others (1972) and Weiblen and Morey (1975) have compared the chemistry of the Logan intrusions with lavas elsewhere.

The changes in composition with height in sills A and B are shown in Figure 26. The medium-grained zone of sill A has a fairly constant composition throughout, which is different from the lower chilled margin and the coarse-grained zone. Compared to the medium-grained zone, the lower chilled margin is richer in SiO_2, but is poorer in total Fe, CaO, and K_2O, and the coarse-grained zone is richer in SiO_2, Fe_2O_3, Na_2O, and K_2O, but is poorer in Al_2O_3, FeO, CaO, MgO, and TiO_2.

It is not as easy to generalize about sill B (fig. 26b), in part because there are only two samples to represent the three medium-grained zones and none from the coarse-grained zone. The most distinctive zone is the porphyry zone which is higher in Al_2O_3, K_2O, and Na_2O (reflecting the abundance of alkali-rich feldspar) and lower in Fe, CaO, MgO, and TiO_2 than other zones. Both upper and lower chilled margins are relatively high in SiO_2 and P_2O_5 and low in Al_2O_3, CaO, and MgO. Figure 27 shows the changes in normative mineralogy with height in sill.

MINERAL CHEMISTRY

Analyses were made on an automated 9-spectrometer Applied Research Laboratories model SEMG electron microprobe at Virginia Polytechnic Institute and State University. They were conducted with an operating voltage of 15 kV and a sample current of 10 μ amp. Data were reduced by the Bence-Albee (1968) method. Selected analyses of feldspar, pyroxene, olivine, biotite, and amphibole are given in Tables A-2, A-3, A-4, A-5, and A-6, respectively. The data for pyroxene and amphibole were treated using the computer programs of Papike and others (1974); analyses presented here were selected on the basis of those programs. The analyses of feldspar, olivine, and biotite were chosen on the basis of the sum of oxides and the need to illustrate a particular composition.

Plagioclase

The plagioclase in all but the coarse-grained zones of the four sills falls within the composition range An_{30} to An_{60}, and most is between An_{42} and An_{54} (table A-2). The plagio-

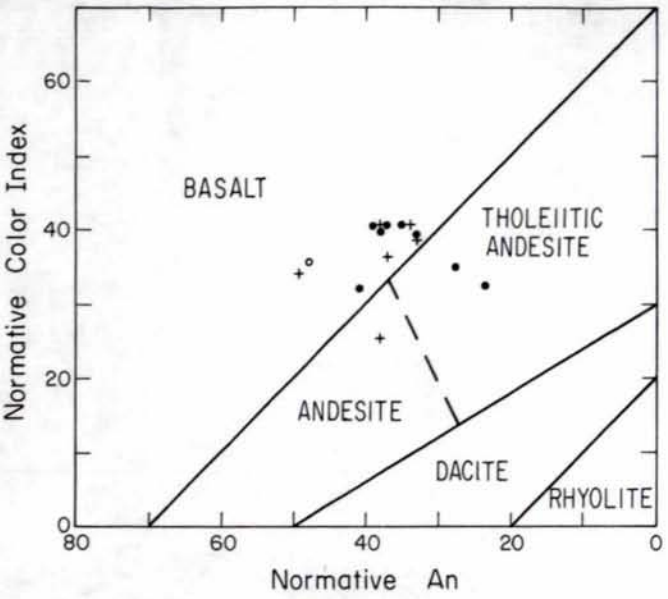

Figure 24. Cation normative color index vs cation normative An with dividing lines for distinguishing subalkaline rocks (after Irvine and Baragar, 1971); •, sill A; + sill B; o, sill D. Most samples are basalts; the two tholeiitic andesites from sill A are from the coarse-grained zone, and the andesite from sill B is from the porphyry zone.

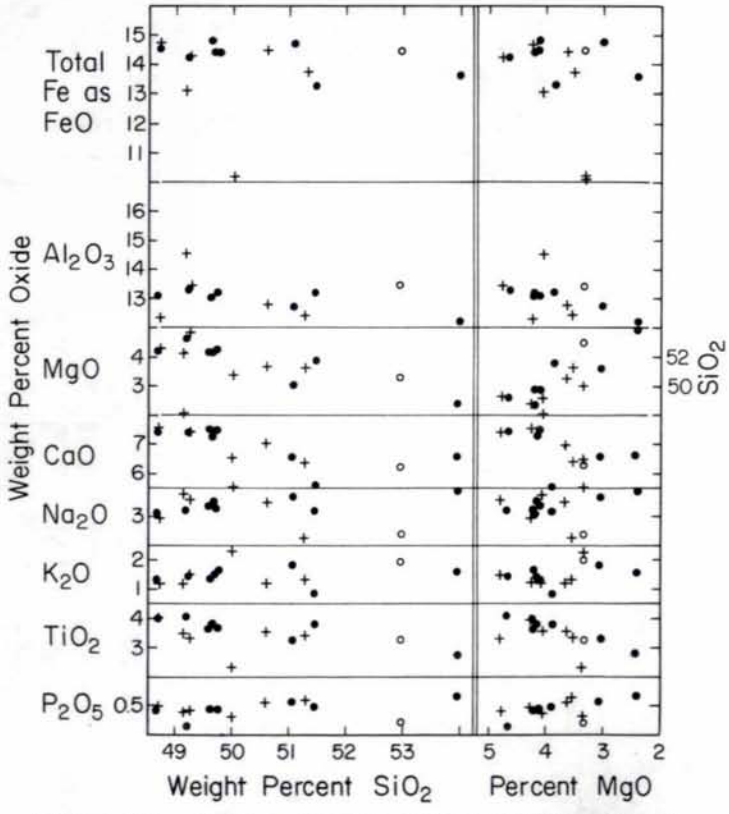

Figure 25. Weight percent oxides vs SiO_2 (left) and MgO. All analyses plotted; •, sill A; +, sill B; o, sill D. The plus marks at 50 percent SiO_2 and 3.34 percent MgO represent the porphyry from sill B.

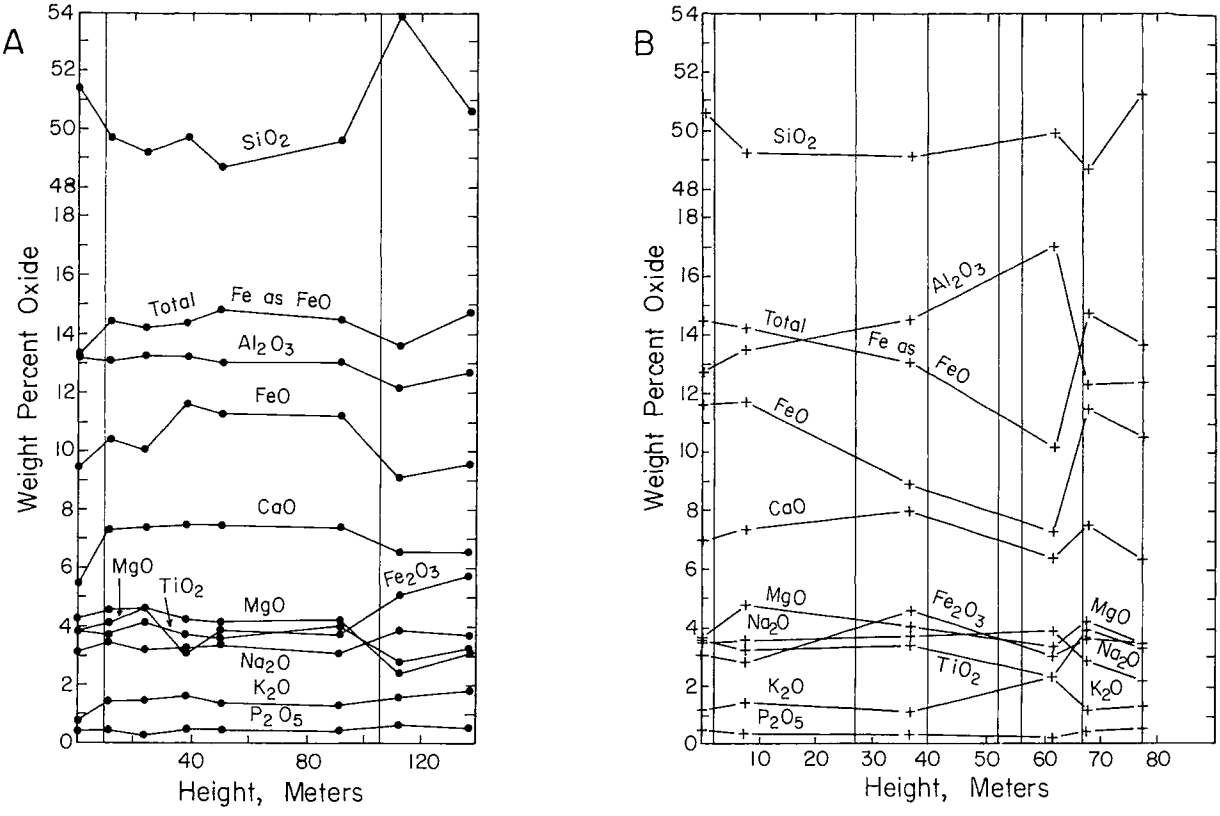

Figure 26. Weight percent oxides vs height in sills A and B. Textural zone boundaries are indicated by vertical lines and can be compared with Figure 5. A, zones are: chilled margin and fine-grained, 0-9 m; medium-grained, 9-105 m; coarse-grained, 105-139 m; upper 23 m of sill not represented. B, zones are: chilled margin and fine-grained, 0-2 m; medium-grained ophitic, 2-27 m; medium-grained intergranular, 27-40 m; coarse-grained, 40-52 m; medium-grained subophitic-intergranular, 52-56 m; porphyry, 56-67 m; fine-grained and chilled margin, 67-77 m.

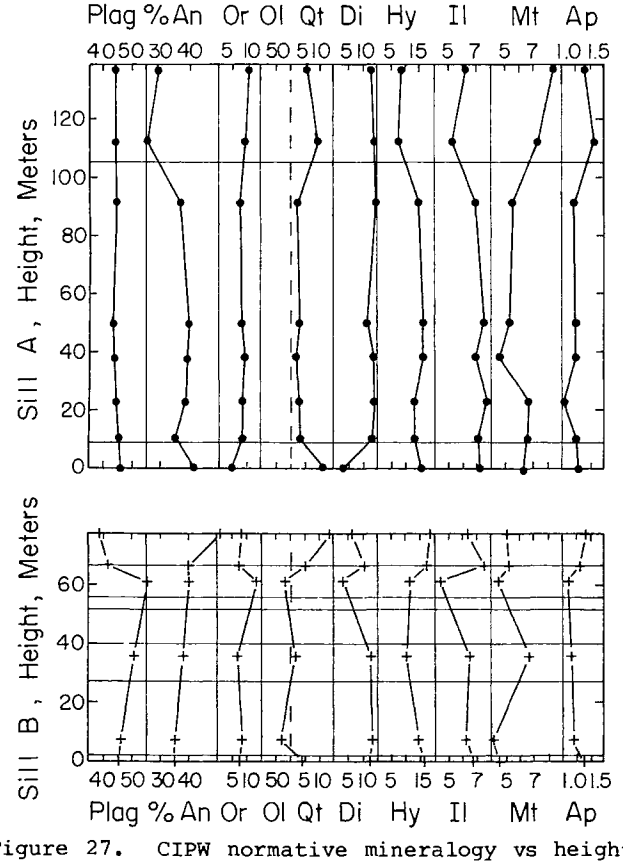

Figure 27. CIPW normative mineralogy vs height in sills A and B. Horizontal lines mark boundaries of textural zones (figs. 5, 26).

clase in the coarse-grained zones is apparently much more sodic (e.g., M11554, M11570).

Plagioclase compositions determined by microprobe are plotted against height in the four sills in Figure 28. Because alteration seems to lower the An content, the maximum value most likely represents the core composition. The maximum An content of the aphyric plagioclase in the lower fine-grained zones is $An_{50.1}$ to $An_{51.3}$; in the medium-grained zones, it is $An_{49.0}$ to $An_{52.1}$; in the coarse-grained zones, $An_{4.1}$ to $An_{8.6}$; and in the porphyry zones, $An_{53.9}$. Phenocrysts from the lower medium-grained zone of sill B and from the fine-grained zone of sill D are more calcic than the matrix plagioclase, and have maximum values of $An_{55.3}$ and $An_{59.1}$, respectively.

The plagioclase in the coarse-grained zone is surprisingly sodic, although the compositions estimated from optical data were no more sodic than those of the other zones. Optically estimated compositions were less than 10 mole percent An higher than the probe determination in the other zones, but were 50 mole percent An higher in the coarse-grained zones. This likely reflects alteration resulting from late-stage concentrations of alkalis and silica in the coarse-grained zones.

An attempt was made to see whether plagioclase varied with textural type. No composi-

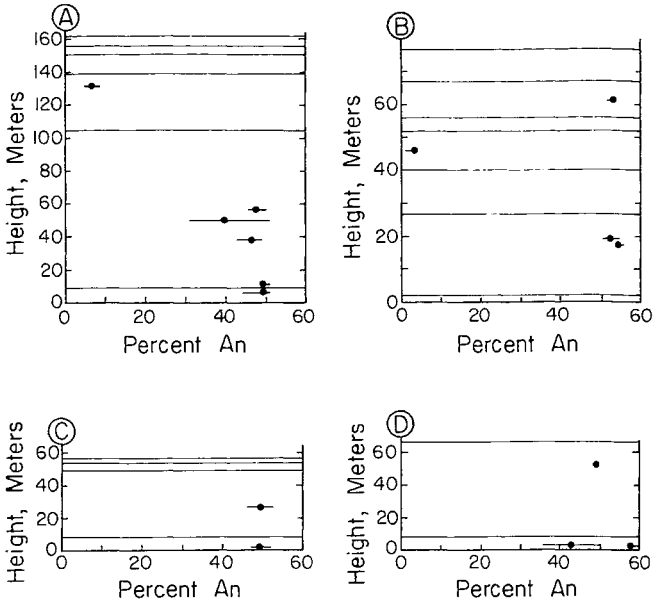

Figure 28. Microprobe-determined An content of plagioclase vs height in sills A, B, C, and D (identified by letters). Dots, average values; lines through dots, range in composition. Horizontal lines mark boundaries of textural zones.

tional differences were detected between plagioclase occurring in ophitic pyroxene and plagioclase occurring in clusters in the same sample. Plagioclase phenocrysts, however, tend to be slightly more calcic than matrix plagioclase.

Pyroxene

Augite is the major pyroxene in all of the samples examined; pigeonite was identified in only a few samples. All reasonable analyses are plotted on Figure 29 in terms of major elements and on Figure 30 in terms of the minor components Ti - NaM_2 - Al^{IV}. In the terminology of Papike and others (1974), most of the pyroxenes are CaMg - TAL, some are NATAL, a few are CaAl - CATS, and one is $CaFe^{2+}$ - TAL. Selected analyses are given in Table A-3.

Figure 31 suggests that single grains of pyroxene are slightly richer in Ca and Fe than composite grains, but there seems to be little difference between single grains showing even and uneven extinction or between the two types of composite grains. Comparison of analyses from the same sample indicates that the range of pyroxene composition in a given sample does not reflect the textural type of pyroxene. The limited data show that single grains with even extinction have a composition spread as large as the other three types of pyroxene.

Although clearly based on inadequate data, Figure 32 suggests that there are no regular compositional changes with height and no compositional distinction between textural zones. The same observation was made by Mathez (1971) for one of the Rose Lake sills.

Olivine

Olivine occurs only in minor amounts in a few samples. It is most abundant in sills A and B, was noted in one sample from sill C, and was not observed in sill D. Analyses from two samples, one from sill A and one from sill B, are given in Table A-4. Although the oxide sums are greater than 100 percent and the stoichiometric balance is not particularly good, it is evident that the olivines are quite iron-rich, averaging $Fa_{78.1}$ in sill A and $Fa_{66.5}$ in sill B. The small size and partial alteration of the olivine grains may have led to overestimating the amount of iron.

Biotite

Biotite occurs only as a secondary mineral formed as part of the pyroxene alteration process. Brown, green, and red or reddish-brown varieties all are present, in some cases in the same sample. Analyses are given in Table A-5. Green biotites are Ti-poor and brown biotites are Ti-rich, as many authors have noted. Red biotite is notably poorer in K and richer in Mg and Ca than the other biotites.

Amphibole

Amphibole, like biotite, is derived from alteration of pyroxene. Five analyses from three rock samples are presented in Table A-6. According to the nomenclature scheme of Leake (1978), all but one of the analyzed amphiboles are ferroedenite; the exception is a ferrohornblende, which has slightly less Na in the A site, but otherwise is similar to the rest.

Fe-Ti Oxides

No complete analyses were made of the opaque oxide minerals, nor were any partial analyses made using proper standards. Rough analyses, with silicate standards for Fe and Ti, indicate that Fe and Ti are in roughly equal proportions in all opaques tested. Observations in reflected light of opaques in polished sections prepared for microprobe analyses indicate that only one oxide phase is present. It is concluded that the opaque Fe-Ti oxide is ilmenite and that no magnetite is present.

Quartz-Feldspar Intergrowths

The feldspar that is intergrown with quartz is almost invariably altered, and therefore analyses are suspect. However, five analyses from three samples (e.g., M11521, micrographic, table A-2) indicate that the intergrown feldspar is an alkali feldspar but that it may be K-rich, Na-rich, or intermediate. The analyses back up the microscopic inferences that some quartz intergrowths are with plagioclase and some with K-feldspar.

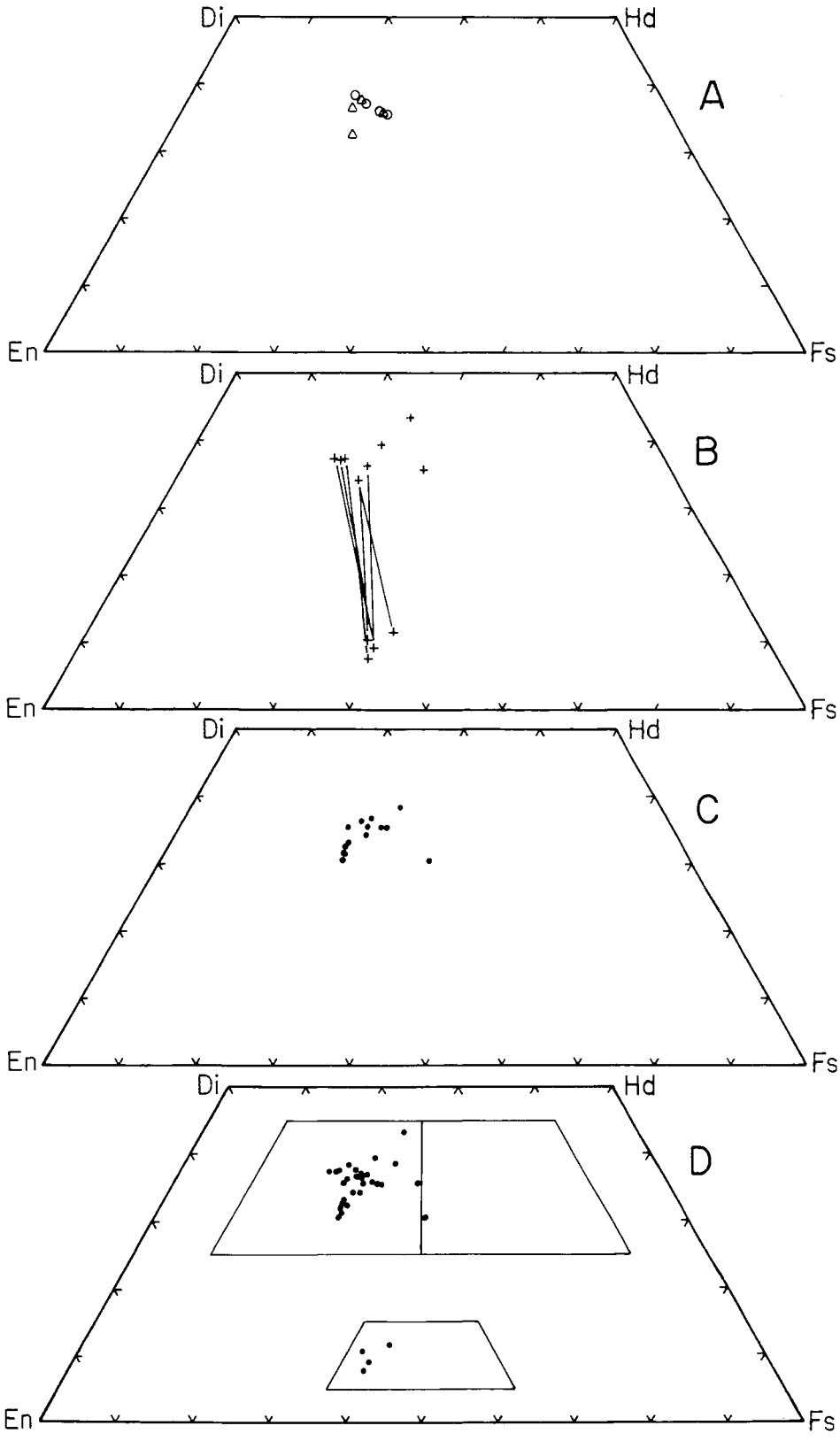

Figure 29. Pyroxene compositions plotted on the pyroxene quadrilateral. A, sills C (open triangles) and D, (open circles); acceptable augite analyses. B, sill B, acceptable augite analyses and pigeonite; tie lines connect coexisting augite and pigeonite. C, sill A; acceptable analyses only. D, composite of all acceptable analyses of augites from sills A, B, C, and D, and of available pigeonite analyses from sill B. Fields delineated are augite (upper left), ferroaugite (upper right), and intermediate pigeonite (lower).

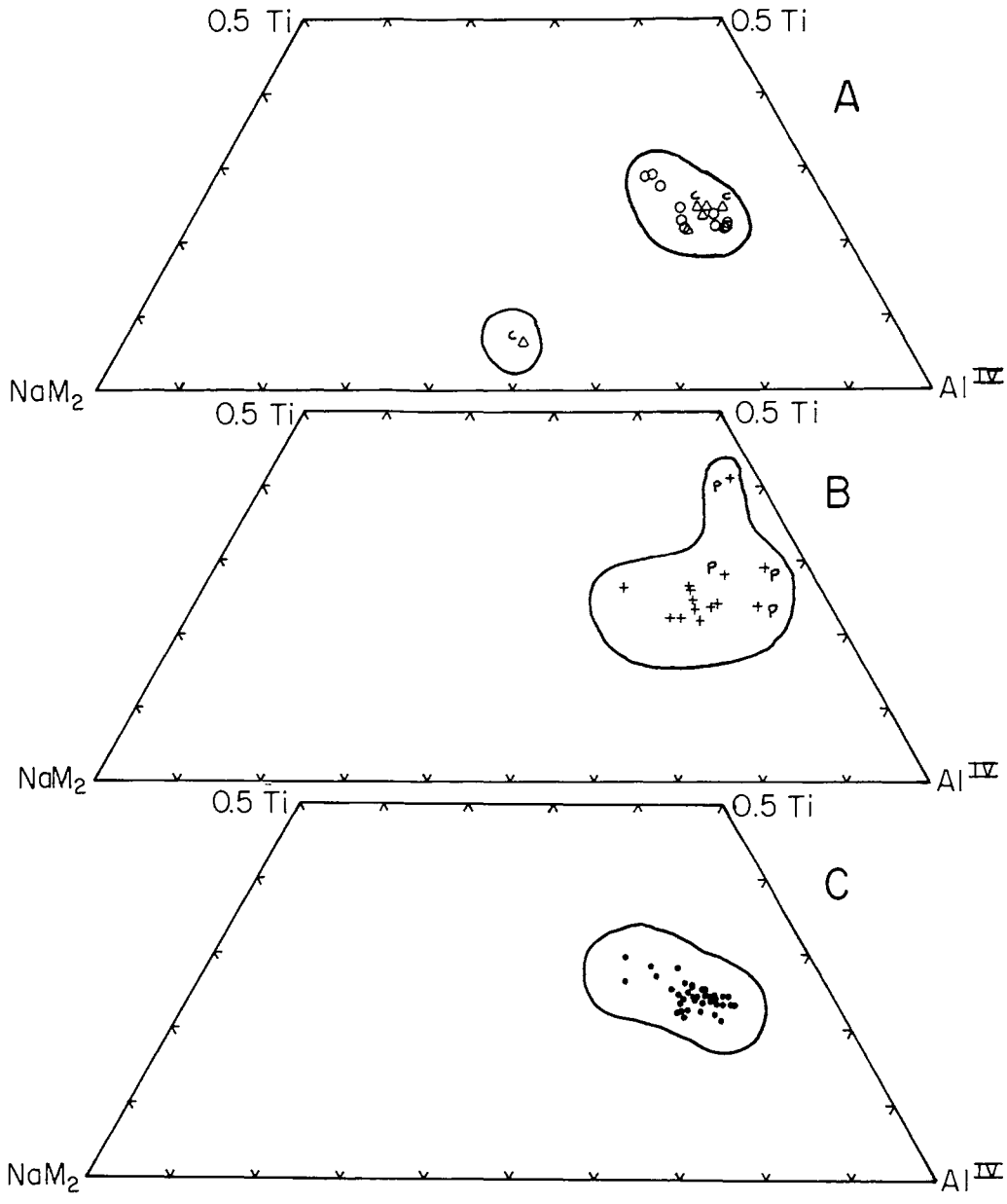

Figure 30. Acceptable analyses of pyroxenes plotted in terms of minor com ponents Ti, Al^{IV} (Al in tetrahedral sites), and NaM_2 (Na in the M_2 site). After Papike and others (1974). A, sill C (open triangles) and sill D (open circles); c, pyroxene poikilitically included in plagioclase. B, sill B; P, pigeonite. C, sill A.

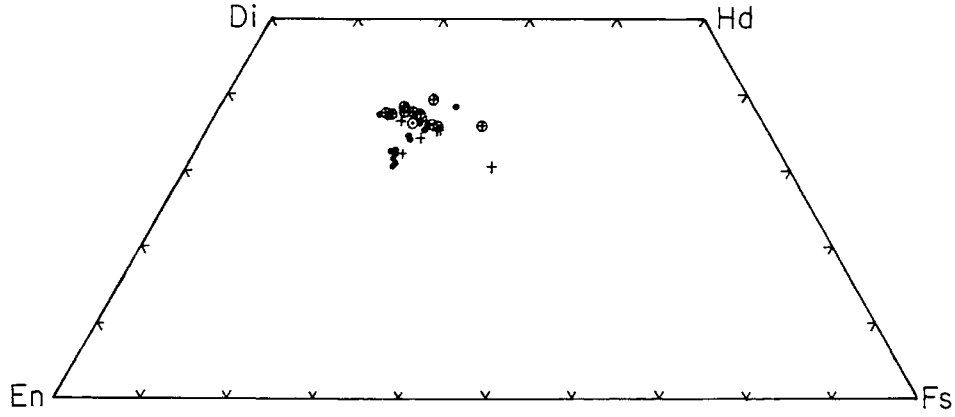

Figure 31. Acceptable augite analyses from all sills plotted on the pyroxene quadrilateral. Plus marks are single grains having even extinction; circled plus marks are single grains having uneven extinction; dots are composite grains in which individuals have similar interference colors; and circled dots are composite grains in which individuals have notably different interference colors.

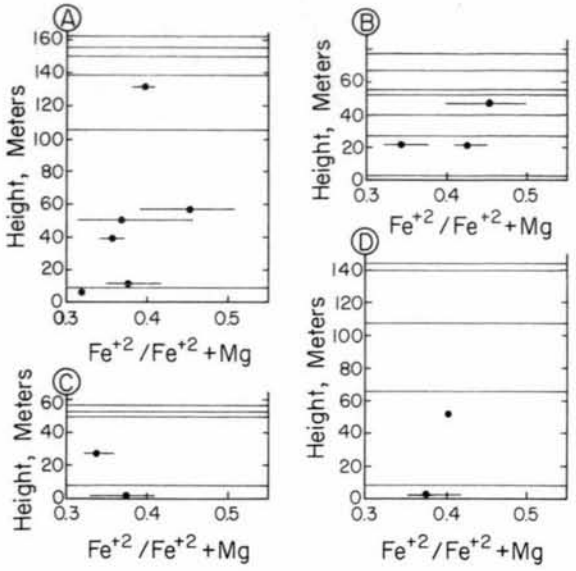

Figure 32. Variation of Fe^{2+}/Fe^{2+} + Mg ratio in pyroxenes with height in sills (identified by letters). Dots represent average values; lines through dots show range in composition. Horizontal lines mark textural zone boundaries. The more iron-rich point near 20 m in sill B is pigeonite; others are augite.

DISCUSSION

The textural relations described above indicate three stages of crystallization: (1) a pre-emplacement stage during which most, if not all of the olivine, some plagioclase, and minor pyroxene and Fe-Ti oxide crystallized; (2) the main crystallization period during which plagioclase, pyroxene, and Fe-Ti oxides coprecipitated, but near the end of which Fe-Ti oxide crystallization may have ceased, and minor crystallization of apatite, quartz, and, in some sills, hornblende and biotite began; and (3) a late-stage crystallization and deuteric alteration period during which quartz-feldspar intergrowths formed, apatite crystallized, and partial alteration of plagioclase to sericite, and pyroxene to hornblende or biotite occurred.

The occurrence of olivine as rounded grains or as rounded glomerocrysts of euhedral grains, its uneven distribution, and the fact that no other primary minerals are included in it although it is included in plagioclase and pyroxene, suggest that it not only preceded other minerals in crystallizing, but that little or no crystallization occurred after emplacement. The glomerocrysts suggest possible disruption of an adcumulate in a magma chamber, or aggregation in a narrow conduit (Vance, 1969); the irregular distribution suggests an inconsistent transport, and the rounding suggests that the olivine was not in equilibrium with the emplaced magma. The Fe-rich nature of the olivine implies that the reservoir magma itself was a fairly evolved magma akin to the upper zone liquid in the Skaergaard layered series (Wager and Brown, 1968), or that considerable reaction occurred during the main crystallization stage.

Plagioclase was obviously on the liquidus at the time of emplacement, as indicated by the presence of phenocrysts in the chilled margins. In ophitic and subophitic diabase, some plagioclase is enclosed in pyroxene and some is accreted in clusters of diversely oriented grains. Since cluster and ophitic plagioclase have the same composition, they must have formed simultaneously. Perhaps the movement of the liquid into interstitial positions coincident with the growth of the large augite crystals caused some of the crystals to drift together. Micrographic intergrowths between quartz and plagioclase suggest the possibility that crystallization of plagioclase continued into the late stage. The few available analyses of this intergrown plagioclase (not in table A-2) indicate that some of it is a K-rich albite.

Most of the pyroxene crystallized during the main crystallization period, but scattered small pyroxene phenocrysts in the chilled margin of sill D indicate some pre-emplacement crystallization. The variability as to single and composite grains can probably be explained in terms of numbers of nuclei in a given area and rates of diffusion toward these nuclei. It seems likely that the diffusion rate was controlled more by the local presence of volatiles than by the cooling rate. Although Lofgren and others (e.g., 1974) have shown that textures of lunar rocks clearly reflect different cooling rates, the fact that pyroxene types seem unrelated to position in the sills suggests that cooling rates were not an overriding factor. The patch-like irregularity of deuteric alteration indicates that volatile distribution varied considerably over small distances. Where volatile concentration was higher, diffusion rates were greater, and single pyroxene grains formed; where fewer volatiles or more nuclei were present, composite grains formed. Perhaps a combination of lower volatile concentration and more nuclei produced composite grains of individuals with dissimilar crystallographic orientations, whereas a combination of higher volatile concentrations and more nuclei produced composite grains of individuals with similar orientations. The similarity in compositional range indicates that the three types cannot be explained on a chemical basis.

The textural variability of the Fe-Ti oxides suggests a complex history. In the chilled margins the acicular, dendritic, and skeletal types, which clearly formed as a result of rapid cooling, display morphologies similar to those described by Usselman and others (1975) for high-titanium mare basalts. The laths and skeletal laths present throughout the sills may be primary ilmenite or they may have formed by the exsolution process described below. The occurrence of grains of type 1 (embayed, holey) and type 2 (skeletal) that are apparently isometric in cross section suggests that the first-formed phase was isometric, but no evidence was found

for an Fe-Ti oxide other than ilmenite and minor hematite.

Following the leads of Buddington and Lindsley (1964), Davidson and Wyllie (1968), and Haggerty (1976), the following possibilities are suggested. An isometric ulvospinel-rich phase crystallized first, as previously suggested by Mathez (1971) and Weiblen and others (1972). This probably occurred early in the crystallization sequence, perhaps even in part before emplacement. Oxidation of type 1 (embayed, holey) oxides occurred early in the sequence, and was followed by exsolution of ilmenite and magnetite. The two segregated from each other with magnetite, the minor phase, forming rounded domains within the ilmenite. Perhaps the higher temperatures in the finer grained zones, where type 1 oxides are more prevalent, promoted migration toward centers rather than toward crystallographic planes. The magnetite was then removed by solution (Davidson and Wyllie, 1968), probably rather quickly, and the holes formed. Continued crystallization of plagioclase and pyroxene then filled the holes (e.g., fig. 14a).

In the coarser grained parts of the sills, exsolution favored migration toward crystallographic planes with segregation of ilmenite along {111} planes of magnetite. Subsequent removal of magnetite was probably contemporaneous with much of the alteration of the previously formed pyroxene crystals and may even have contributed to the formation of some of the secondary Fe-Mg silicates. During removal of magnetite, ilmenite plates were enlarged and distorted from their original shapes.

In most samples, quartz and quartz-feldspar intergrowths crystallized late because they occupy interstitial areas. This quartz and much of the associated feldspar likely crystallized in eutectic-like proportions to produce the wide variety of intergrowth textures. Differing proportions and perhaps differing compositions of volatiles may have contributed significantly to the textural variability. The fact that some of the intergrowths seem to be between quartz and adjoining plagioclase suggests that replacement also played a role in the development of these textures. The presence in a few samples of subhedral quartz that is neither interstitial nor intergrown with feldspar suggests that some quartz may have crystallized during the later part of the main crystallization sequence.

Most of the apatite is associated with interstitial quartz and thus also crystallized late in the sequence, although apatite included in plagioclase and pyroxene must have crystallized near the end of the main crystallization stage.

Characteristic of these sills is the large amount of alteration and the variability in intensity of alteration even on the scale of a thin section (e.g., fig. 9c). The most altered mineral is pyroxene. It is suggested that the marginal alteration was produced as a typical reaction rim late in the main crystallization stage or perhaps early in the late stage, whereas the other types were formed entirely during the late stage. The role of volatiles is indicated by the relation of alteration to cleavage and by the uneven distribution of patches of pyroxene (Weiblen and others, 1972). The occurrence of minor amounts of euhedral biotite and amphibole in sill A, the thickest sill, suggests that the partial pressure of water may have been sufficient to allow direct precipitation of these hydrous phases (Yoder and Tilley, 1962; Weiblen and others, 1972).

Development of Textural Zones

Mineralogy, texture, and chemistry indicate that the textural zones of the four sills resulted from intrusion of a crystal-bearing magma which cooled from the margins inward. Although plagioclase crystals contained in the magma were concentrated in porphyritic zones, most other major minerals formed by crystallization after intrusion and remained evenly dispersed. Grain size is smallest where cooling was rapid, and is largest in the central parts of the sills where cooling was slow and volatiles became concentrated as crystallization progressed.

It is evident, however, from Table 2 and Figure 5 that within the major textural zones there are a variety of fabrics. Three of these fabrics--ophitic, poikilitic, and intergranular--reflect relationships between plagioclase and pyroxene. An intergranular fabric clearly implies simultaneous crystallization of the two phases, but the implications of ophitic and poikilitic fabrics are less clear.

Ophitic textures have been interpreted in several ways. Several authors (e.g., see discussion in Bowen, 1928, p. 68-69; Wager, 1961; Engelhardt, 1979) consider that because plagioclase is included in pyroxene, crystallization of plagioclase must have begun well before that of pyroxene. Others (e.g., Bowen, 1928) believe that crystallization of the two was simultaneous. Simultaneous crystallization of plagioclase and pyroxene can result in ophitic textures because at a given degree of undercooling, plagioclase nucleates rapidly but grows slowly, and pyroxene nucleates slowly but grows rapidly and envelops the smaller plagioclase crystals (Carmichael and others, 1974; Kirkpatrick, 1976). Cox and others (1979) believe that ophitic textures develop when simultaneous crystallization of plagioclase and pyroxene is preceded by crystallization of some plagioclase. This seems to be the best explanation for the development of ophitic texture in the sills, because, as previously indicated, at least some plagioclase began to crystallize before pyroxene.

If plagioclase began to crystallize before pyroxene in the four sills studied, why are there fabrics other than ophitic? In the chilled margins and fine-grained zones, one can assume that rapid cooling and a high degree of under-

cooling brought both plagioclase and pyroxene below the maxima in the growth-rate curves so that both nucleated and grew simultaneously at similar rates. But what about the coarse-grained zones which also have intergranular textures? Perhaps differences in volatile content influenced the relative positions of maxima on growth-rate curves. Or perhaps the nature of seed crystals in the melt when these zones formed had some influence. Experiments by Nabelek and others (1978) show that textures are greatly influenced by the size and shape of the crystals in the melt just before cooling. In experiments with lunar analogs they were able to produce intersertal, porphyritic, and poikilitic textures from chemically identical charges cooled at the same rate, but having different pre-cooling histories.

A poikilitic texture was observed only in the lower fine-grained zone in sill C. Mathez (1971) found it in upper and lower fine-grained zones in both of the Rose Lake sills which also are thin sills, averaging 25.3 and 21.9 m. Possibly this texture developed only in fine-grained zones of thin Logan sills. If so, it would seem largely a result of cooling rates and degree of undercooling, and possibly also a result of the nature of the crystals in the melt having been somehow controlled by flow segregation in the conduits which fed these smaller sills.

The origin of the porphyry zones has been discussed by Grout and Schwartz (1933) and in some detail by Mathez (1971). Grout and Schwartz (1933) regarded flotation or sinking as the most favorable explanation for segregation of plagioclase. Mathez (1971), however, concluded that the porphyry zones in the Rose Lake sills could best be explained as a combination of multiple intrusions and flow differentiation, whereby a more viscous, phenocryst-rich liquid was emplaced above previously emplaced, less viscous liquids.

CONCLUSIONS

Quartz-normative tholeiitic magmas containing phenocrysts of plagioclase and, in some magmas, minor olivine, were emplaced as sills in the Rove Formation during middle Proterozoic time. The presence of xenocrysts of quartz and xenoliths of Rove Formation, and the higher SiO_2 content of the chilled margins of sills A and B suggest some assimilation of the host Rove Formation. Crystallization of the magma proceeded inward from the margins at decreasing cooling rates. Variable cooling rates, different degrees of undercooling, and perhaps variety in type of suspended seed crystals resulted in different plagioclase-pyroxene fabrics. The monotonous chemistry and mineralogy throughout the fine- and medium-grained zones indicates that there was little gravity segregation of phases as they precipitated in these zones. Plagioclase crystals suspended in the intruded liquid were either trapped in the crystallizing liquid as scattered phenocrysts or were concentrated to form the porphyry zones. Silica, alkalis, and water were enriched in the final liquids. Much of this liquid was trapped in crystal meshes throughout the sills and finally crystallized to micrographic intergrowths of quartz and feldspar. However, a significant amount of the liquid migrated toward the zone that crystallized last, and strongly influenced its final consolidation. Thus in the coarse-grained zones, the feldspars are notably more alkali-rich than in other zones, quartz-feldspar intergrowths are especially abundant, pyroxenes are almost completely altered, and alteration pervades most of the rock.

ACKNOWLEDGMENTS

This project was begun with support for field work and thin sections from the Minnesota Geological Survey; subsequent support came from a faculty development grant from the University of Wisconsin at Oshkosh. Microprobe time was generously donated by the Department of Geological Sciences, Virginia Polytechnic Institute and State University, Blacksburg, Virginia. I am grateful to each of these organizations and to my wife Judy for their support.

REFERENCES CITED

Beck, M.E., 1970, Paleomagnetism of Keweenawan intrusive rocks, Minnesota: Journal of Geophysical Research, v. 75, p. 4985-4996.

Beck, M.E., and Lindsley, N.C., 1969, Paleomagnetism of the Beaver Bay Complex, Minnesota: Journal of Geophysical Research, v. 74, p. 2002-2013.

Bence, A.E., and Albee, A.L., 1968, Empirical correction factors for the electron microanalysis of silicates and oxides: Journal of Geology, v. 76, p. 382-403.

Bowen, N.L., 1928, The evolution of the igneous rocks: New York, Dover Publications, 332 p.

Buddington, A.F., and Lindsley, D.H., 1964, Iron-titanium oxide minerals and synthetic equivalents: Journal of Petrology, v. 5, p. 310-357.

Carmichael, I.S.E., Turner, F.J., and Verhoogen, J., 1974, Igneous petrology: McGraw-Hill, 739 p.

Chase, C.G., and Gilmer, T.H., 1973, Precambrian plate tectonics: the Midcontinent Gravity High: Earth and Planetary Science Letters, v. 21, p. 70-78.

Cox, K.G., Bell, J.D., and Pankhurst, R.J., 1979, The interpretation of igneous rocks: London, George Allen and Unwin, 450 p.

Davidson, A., and Wyllie, P.J., 1968, Opaque oxide minerals of some diabase-granophyre

associations in Pennsylvania: Economic Geology, v. 63, p. 950-960.

Du Bois, P.M., 1962, Paleomagnetism and correlation of Keweenawan rocks: Geological Survey of Canada Bulletin 71, 75 p.

Engelhardt, W.V., 1979, Ilmenite in the crystallization sequence of lunar rocks: Lunar and Planetary Science Conference, 10th, Proceedings, p. 677-694.

Geul, J.J.C., 1970, Geology of Devon and Pardee Townships and the Stuart location: Ontario Department of Mines and Geology Report 87, 52 p.

Grant, J.A., 1970, Geology of northern part of Gunflint Lake quadrangle, in Sims, P.K., and Westfall, I., eds., Summary of field work, 1970: Minnesota Geological Survey Information Circular 8, p. 20.

Green, J.C., 1972, North Shore Volcanic Group, in Sims, P.K., and Morey, G.B., eds., Geology of Minnesota: a centennial volume: Minnesota Geological Survey, p. 294-332.

Grout, F.F., and Schwartz, G.M., 1933, The geology of the Rove Formation and associated intrusives in northeastern Minnesota: Minnesota Geological Survey Bulletin 24, 103 p.

Haggerty, S.E., 1976, Oxidation of opaque mineral oxides in basalts, in Rumble, D., III, Oxide minerals, v. 3: Mineralogical Society of America, Short Course Notes, p. Hg1-Hg100.

Irvine, T.N., and Baragar, W.R.A., 1971, A guide to the chemical classification of the common volcanic rocks: Canadian Journal of Earth Sciences, v. 8, p. 523-548.

Jahn, Bor-ming, Bernard-Griffiths, J., Charlot, R., Cornichet, J., and Vidal, F., 1980, Nd and Sr isotopic compositions and REE abundances of Cretaceous MORB (holes 417D and 418A, legs 51, 52, and 53): Earth and Planetary Science Letters, v. 48, p. 171-184.

Kirkpatrick, R.J., 1976, Towards a kinetic model for the crystallization of magma bodies: Journal of Geophysical Research, v. 81, p. 2565-2571.

Lawson, A.C., 1893, Laccolithic sills of the north-west coast of Lake Superior: Geological and Natural History Survey of Minnesota Bulletin 8, p. 24-48.

Leake, B.E., 1978, Nomenclature of amphiboles: American Mineralogist, v. 63, p. 1023-1052.

Le Maitre, R.W., 1976, The chemical variability of some common igneous rocks: Journal of Petrology, v. 17, p. 589-637.

Lofgren, G., Donaldson, C.H., Williams, R.J., Mullins, O., Jr., and Usselman, T.M., 1974, Experimentally reproduced textures and mineral chemistry of Apollo 15 quartz normative basalts: Lunar Science Conference, 5th, Proceedings, p. 549-567.

Mathez, E.A., 1971, Geology and petrology of the Logan intrusives of the Hungry Jack Lake quadrangle, Cook County, Minnesota: Unpublished M.S. thesis, University of Arizona, 111 p.

Mathez, E.A., Nathan, H.D., and Morey, G.B., 1977, Geologic map of the Hungry Jack Lake quadrangle, Cook County, Minnesota: Minnesota Geological Survey Miscellaneous Map M-39.

Morey, G.B., 1965, The sedimentology of the Precambrian Rove Formation in northeastern Minnesota: Unpublished Ph.D. dissertation, University of Minnesota, 292 p.

_____1969, The geology of the Middle Precambrian Rove Formation in northeastern Minnesota: Minnesota Geological Survey Special Publication SP-7, 62 p.

Morey, G.B., and Nathan, H.D., 1977, Geologic map of the South Lake quadrangle, Cook County, Minnesota: Minnesota Geological Survey Miscellaneous Map M-38.

_____1978, Geologic map of the Gunflint Lake quadrangle, Cook County, Minnesota: Minnesota Geological Survey Miscellaneous Map M-42.

Morey, G.B., Weiblen, P.W., Papike, J.J., and Anderson, D.H., 1981, Geologic map of the Long Island Lake quadrangle, Cook County, Minnesota: Minnesota Geological Survey Miscellaneous Map M-46.

Mudrey, M.G., Jr., 1973, Structure and petrology of the sill on Pigeon Point, Cook County, Minnesota: Unpublished PH.D. dissertation, University of Minnesota, 310 p.

Nabelek, P.I., Taylor, L.A., and Lofgren, G.E., 1978, Nucleation and growth of plagioclase and the development of textures in a high-alumina basaltic melt: Lunar and Planetary Science Conference, 9th, Proceedings, p. 725-741.

Nathan, H.D., 1969, The geology of a portion of the Duluth Complex, Cook County: Unpublished Ph.D. dissertation, University of Minnesota, 198 p.

Palmer, H.C., 1970, Paleomagnetism and correlation of some Middle Keweenawan rocks, Lake Superior: Canadian Journal of Earth Sciences, v. 7, p. 1410-1436.

Papike, J.J., Cameron, K.L., and Baldwin, K., 1974, Amphiboles and pyroxenes: characterization of other than quadrilateral components and estimates of ferric iron from microprobe data [abs.]: Geological Society of America Abstracts with Programs, v. 6, no. 7, p. 1053-1054.

Robertson, W.A., and Fahrig, W.F., 1971, The great paleomagnetic loop--the polar wandering path from Canadian Shield rocks during the Neohelikian Era: Canadian Journal of Earth Sciences, v. 8, p. 1355-1372.

Sims, P.K., 1970, Geologic map of Minnesota, bedrock geology: Minnesota Geological Survey Miscellaneous Map M-14, scale 1:1,000,000.

Usselman, T.M., Lofgren, G.E., Donaldson, C.H., and Williams, R.J., 1975, Experimentally reproduced textures and mineral chemistry of high-titanium mare basalts: Lunar Science Conference, 6th, Proceedings, p. 997-1020.

Vance, J.A., 1969, On synneusis: Contributions to Mineralogy and Petrology, v. 24, p. 7-29.

Wager, L.R., 1961, A note on the origin of ophitic texture in the chilled olivine gabbro of the Skaergaard intrusion: Geological Magazine, v. 98, p. 353-366.

Wager, L.R., and Brown, G.M., 1968, The Skaergaard intrusion, east Greenland, in Layered igneous rocks: London, Oliver and Boyd, p. 11-246.

Weiblen, P.W., Mathez, E.A., and Morey, G.B., 1972, Logan intrusions, in Sims, P.K., and Morey, G.B., eds., Geology of Minnesota: a centennial volume: Minnesota Geological Survey, p. 394-406.

Weiblen, P.W., and Morey, G.B., 1975, The Duluth Complex--a petrologic and tectonic summary: American Institute of Mining, Metallurgical and Petroleum Engineers, Minnesota Section, 48th Annual Meeting, Proceedings, p. 72-95.

Weiblen, P.W., and Morey, G.B., 1980, A summary of the stratigraphy, petrology, and structure of the Duluth Complex: American Journal of Science, v. 280-A, pt. 1, p. 88-133.

Yoder, H.S., Jr., and Tilley, C.E., 1962, Origin of basalt magmas: an experimental study of natural and synthetic rock systems: Journal of Petrology, v. 3, p. 342-532.

Table A-1. Chemical analyses and CIPW norms
[Analyses by Tamiya Asari, Japan Analytical Chemistry Consultants Co. Ltd., in 1972]

					Sill A								Sill B				Sill D
Sample	M11516	M11521	M11531	M11539	M11621	M11545	M11551	M11555	Whole Sill	M11556	M11561	M11568	M11575	M11578	M11585	Whole Sill	M11586
Height (m)	0	10.7	23.5	38.1	50	91.7	112.2	137.2		0	7.6	36.6	61.6	67.7	77.4		0
SiO_2	51.46	49.67	49.19	49.72	48.68	49.62	53.95	51.06	50.1	50.61	49.27	49.17	50.00	48.72	51.29	49.8	52.95
TiO_2	3.80	3.72	4.09	3.68	3.97	3.67	2.78	3.25	3.6	3.54	3.30	3.46	2.32	3.96	3.40	3.3	3.23
Al_2O_3	13.20	13.09	13.26	13.19	13.03	13.02	12.18	12.71	13.1	12.75	13.44	14.55	17.11	12.34	12.43	13.9	13.48
Fe_2O_3	4.29	4.52	4.64	3.12	3.70	3.82	5.03	5.74	4.2	3.06	2.81	4.67	3.08	3.66	3.54	3.8	2.21
FeO	9.45	10.40	10.06	11.61	11.19	11.37	9.12	9.59	10.5	11.69	11.72	8.90	7.37	11.49	10.53	10.1	12.50
CaO	5.46	7.30	7.36	7.46	7.43	7.48	6.58	6.55	7.2	6.98	7.38	8.05	6.45	7.57	6.38	7.3	6.23
MgO	3.83	4.16	4.66	4.21	4.21	4.14	2.41	3.04	3.9	3.65	4.79	4.07	3.34	4.23	3.52	4.0	3.33
MnO	0.15	0.15	0.17	0.16	0.17	0.16	0.18	0.17	0.16	0.14	0.16	0.14	0.12	0.16	0.14	0.15	0.14
Na_2O	3.15	3.50	3.19	3.22	3.10	3.37	3.90	3.69	3.4	3.48	3.55	3.73	3.95	2.97	2.23	3.6	2.39
K_2O	0.81	1.42	1.47	1.62	1.36	1.35	1.59	1.82	1.5	1.21	1.47	1.19	2.36	1.26	1.37	1.5	1.98
H_2O (+)	2.52	1.04	1.73	1.35	1.55	1.32	1.13	1.67	1.4	1.88	1.42	1.33	2.59	1.85	3.08	1.6	1.48
H_2O (-)	1.02	0.82	0.72	0.91	1.21	0.92	0.95	0.91	0.9	1.03	0.80	0.81	1.12	1.28	1.10	0.9	0.51
P_2O_5	0.47	0.44	0.22	0.43	0.42	0.41	0.66	0.56	0.43	0.54	0.40	0.38	0.31	0.49	0.59	0.43	0.20
CO_2	0.08	0.26	0.00	0.09	0.42	0.02	0.09	0.00	0.15	0.06	0.21	0.22	0.64	0.77	0.93	0.34	0.02
Total	99.69	100.49	100.76	100.77	100.44	100.67	100.55	100.62	100.08	100.62	100.72	100.67	100.76	100.75	100.53	100.8	100.65
Q	11.48	3.09	2.97	1.73	3.44	2.28	9.41	5.56	3.8	4.21	--	1.66	--	4.97	13.77	2.0	8.46
or	4.79	8.39	8.69	9.57	8.04	7.98	9.40	10.76	8.9	7.15	8.69	7.03	13.95	7.45	8.10	8.9	11.70
ab	26.66	29.62	26.99	27.25	26.23	28.52	33.00	31.23	28.8	29.45	30.04	31.56	33.43	25.13	18.87	30.5	20.22
an	19.49	15.81	17.52	16.75	17.62	16.41	11.03	12.74	16.1	15.60	16.40	19.44	21.99	16.62	19.86	17.3	20.21
di	3.31	13.11	14.36	14.07	11.48	14.88	14.00	13.33	13.2	12.68	13.54	13.59	3.25	10.69	1.72	11.5	7.84
hy	15.72	13.39	12.78	16.43	16.04	14.86	7.32	8.78	13.3	16.08	14.85	10.52	11.47	17.05	18.97	14.5	20.38
ol	---	---	---	---	---	---	---	---	---	---	3.24	--	1.93	---	---	---	---
mt	6.22	6.55	6.73	4.52	5.36	5.54	7.29	8.32	6.1	4.44	4.07	6.77	4.47	5.31	5.13	5.5	3.20
il	7.22	7.07	7.77	6.99	7.54	6.97	5.28	6.17	6.8	6.72	6.27	6.57	4.41	7.52	6.46	6.3	6.13
ap	1.09	1.02	0.51	1.00	0.97	0.95	1.53	1.30	1.0	1.25	0.93	0.88	0.72	1.14	1.37	1.0	0.46
cc	0.18	0.59	--	0.20	0.96	0.05	0.20	--	0.34	0.14	0.48	0.50	1.46	1.75	2.12	0.77	0.05

Table A-2. Selected microprobe analyses of feldspar

	Sill A										Sill B			Sill C			Sill D	
Sample	M11616	M11521 ophite	M11521 cluster	M11521 micro-graphic	M11621 single grain	M11621 ophite	M11623a	M11554	M11566	M11566	M11566 pheno-cryst	M11570	M11575 pheno-cryst	M11625 oiko-cryst	M11627	M11631 core	M11631 rim	M11631 pheno-cryst
Height (m)	6.1	10.7	10.7	10.7	50.0	50.0	56.7	131.4	21.6	21.6	21.6	45.4	61.6	1.5	27.4	2.1	2.1	2.1
Major oxides, weight percent																		
SiO_2	56.5	56.4	56.9	65.3	57.6	60.3	57.0	64.7	54.9	56.5	54.8	65.9	54.4	55.8	55.2	56.3	59.1	53.8
TiO_2	0.54	0.47	0.45	0.42	0.09	0.03	0.05	0.36	0.09	0.10	0.11	0.18	0.10	0.14	0.13	0.11	0.05	0.09
Al_2O_3	25.6	25.3	26.2	17.4	24.6	23.6	25.8	18.7	27.3	27.2	27.1	18.7	26.8	25.5	26.6	26.0	24.2	27.8
FeO	0.09	0.5	0.6	0.00	0.66	0.53	0.61	0.00	0.81	0.51	0.67	0.76	0.52	0.95	0.83	0.68	0.51	0.61
MgO	0.14	0.14	0.13	0.04	0.14	0.06	0.10	0.03	0.18	0.11	0.12	0.05	0.12	0.20	0.12	0.16	0.16	0.14
CaO	10.75	10.27	10.35	0.29	9.35	6.96	9.07	1.64	11.4	10.6	10.7	0.52	11.1	10.6	10.7	10.14	7.89	12.1
MnO	0.04	0.02	0.04	0.03	0.00	0.00	0.00	0.01	0.00	0.00	0.00	0.00	0.00	0.00	0.00	0.00	0.00	0.00
Na_2O	5.46	5.72	5.80	3.68	6.3	7.4	5.7	9.57	4.96	5.3	4.79	10.6	5.4	5.6	5.2	5.4	7.1	5.0
K_2O	0.28	0.34	0.31	11.08	0.42	0.44	0.44	1.50	0.30	0.36	0.28	0.05	0.31	0.27	0.32	0.28	0.35	0.24
Total	100.2	99.2	100.8	98.2	99.1	99.4	98.8	96.5	99.89	100.7	98.6	96.7	98.7	99.1	99.1	99.2	99.26	99.3
Molecular proportions, O = 8																		
Si	2.553	2.570	2.551	3.019	2.619	2.714	2.593	2.956	2.491	2.533	2.509	2.985	2.499	2.550	2.519	2.561	2.668	2.457
Al	1.365	1.357	1.385	0.948	1.318	1.251	1.382	1.008	1.458	1.435	1.463	0.996	1.449	1.376	1.433	1.395	1.287	1.498
Fe	0.033	0.019	0.022	0.000	0.025	0.020	0.023	0.000	0.031	0.019	0.025	0.029	0.020	0.036	0.032	0.026	0.019	0.023
Ti	0.018	0.016	0.015	0.015	0.003	0.001	0.002	0.012	0.003	0.003	0.003	0.006	0.003	0.005	0.004	0.004	0.002	0.003
Mg	0.009	0.009	0.009	0.003	0.009	0.004	0.007	0.002	0.012	0.007	0.008	0.004	0.008	0.013	0.008	0.011	0.011	0.009
Mn	0.002	0.001	0.001	0.001	0.000	0.000	0.000	0.000	0.000	0.000	0.000	0.000	0.000	0.000	0.000	0.000	0.000	0.000
Ca	0.520	0.501	0.497	0.014	0.456	0.335	0.442	0.080	0.554	0.507	0.524	0.025	0.544	0.520	0.523	0.494	0.382	0.594
Na	0.478	0.505	0.503	0.330	0.553	0.646	0.502	0.848	0.437	0.462	0.425	0.930	0.480	0.497	0.462	0.477	0.620	0.398
K	0.016	0.020	0.018	0.653	0.024	0.025	0.026	0.087	0.017	0.020	0.017	0.003	0.018	0.016	0.018	0.016	0.020	0.014
Total	4.994	4.998	5.001	4.953	5.007	4.996	4.977	4.993	5.003	4.986	4.974	4.978	5.021	5.013	4.999	4.984	5.009	4.996
Feldspar components, mole percent																		
Or	1.58	1.95	1.77	65.50	2.32	2.49	2.68	8.57	1.69	2.02	1.76	0.31	1.73	1.55	1.79	1.62	1.96	1.39
Ab	47.14	49.22	49.41	33.10	53.53	64.21	51.75	83.55	43.35	46.71	44.00	97.08	46.07	48.11	46.06	48.33	60.67	39.56
An	51.28	48.83	48.82	1.40	44.14	33.30	45.57	7.88	54.96	51.26	54.24	2.61	52.21	50.34	52.14	50.05	37.38	59.05

Table A-3. Selected microprobe analyses of pyroxene
[Fe^{3+} estimated using methods of Papike and others (1974)]

	Sill A				Sill B					Sill C		Sill D	
Sample	M11521	M11621	M11621	M11623a	M11554	M11566	M11566	M11566*	M11570	M11625	M11627	M11631	M11631
Height (m)	10.7	50.0	50.0	56.7	131.4	21.6	21.6	21.6	45.4	1.5	27.4	2.1	2.1
Major oxides, weight percent													
SiO_2	51.2	50.5	51.4	50.3	50.3	51.3	51.3	51.1	50.2	50.9	51.6	50.7	51.0
TiO_2	1.31	0.73	1.05	0.69	1.29	0.87	0.91	0.46	0.65	1.25	0.95	0.75	0.93
Al_2O_3	1.80	1.28	1.97	1.14	1.64	1.55	1.88	0.66	1.07	2.13	1.80	1.32	1.37
FeO	15.1	17.5	14.8	22.0	15.9	15.7	13.1	23.1	18.9	16.0	14.4	17.3	14.1
MgO	15.5	11.5	15.2	11.6	13.6	14.2	14.3	18.3	10.8	14.9	13.8	12.7	13.7
CaO	14.6	18.0	15.5	14.4	16.0	16.5	17.9	5.13	16.6	15.4	18.1	16.8	18.2
MnO	0.30	0.25	0.18	0.30	0.38	0.22	0.21	0.31	0.35	0.21	0.22	0.26	0.19
Na_2O	0.29	0.21	0.24	0.18	0.35	0.29	0.30	0.04	0.22	0.25	0.22	0.25	0.26
K_2O	0.02	0.02	0.02	0.02	0.02	0.01	0.01	0.02	0.00	0.02	0.02	0.02	0.02
Total	100.0	100.0	100.3	100.6	99.6	100.7	100.1	99.2	98.7	101.0	101.1	100.2	99.7
Tetrahedral cations													
Si	1.928	1.943	1.929	1.945	1.924	1.935	1.932	1.958	1.964	1.910	1.933	1.941	1.938
Al^{IV}	0.072	0.057	0.071	0.052	0.074	0.065	0.068	0.030	0.036	0.090	0.067	0.059	0.061
Total	2.000	2.000	2.00	1.997	1.998	2.000	2.000	1.988	2.000	2.000	2.000	2.000	1.999
Octahedral cations													
Al^{VI}	0.008	0.001	0.016	0.000	0.000	0.004	0.015	0.000	0.013	0.005	0.013	0.000	0.000
Fe^{2+}	0.463	0.534	0.451	0.686	0.484	0.462	0.390	0.736	0.616	0.468	0.436	0.521	0.420
Fe^{3+}	0.011	0.030	0.013	0.025	0.026	0.033	0.023	0.006	0.001	0.033	0.016	0.034	0.027
Mg	0.868	0.661	0.851	0.668	0.777	0.799	0.806	1.048	0.628	0.832	0.768	0.725	0.777
Mn	0.010	0.008	0.006	0.010	0.012	0.007	0.007	0.010	0.011	0.007	0.007	0.008	0.006
Ti	0.037	0.021	0.030	0.020	0.037	0.025	0.026	0.013	0.019	0.035	0.027	0.022	0.026
Total	1.397	1.255	1.366	1.409	1.336	1.330	1.266	1.813	1.289	1.379	1.267	1.310	1.257
Ca	0.587	0.744	0.623	0.597	0.655	0.666	0.724	0.211	0.695	0.619	0.726	0.689	0.740
Na	0.021	0.015	0.017	0.013	0.026	0.021	0.022	0.003	0.017	0.018	0.016	0.018	0.019
Total Cations	2.005	2.015	2.006	2.018	2.017	2.016	2.012	2.027	2.001	2.017	2.008	2.017	2.016
Quadrilaterals and others, mole percent													
Quads.	92.80	94.28	92.92	94.81	92.62	93.50	93.17	97.00	96.39	91.02	93.32	94.09	93.88
Others	7.20	5.72	7.08	5.19	7.38	6.50	6.83	3.00	3.61	8.98	6.68	5.91	6.12
Pyroxene components, mole percent													
Wo	30.61	38.36	32.38	30.59	34.18	34.54	37.70	10.56	35.86	32.25	37.61	35.61	38.20
En	45.26	34.08	44.20	34.26	40.58	41.48	41.97	52.55	32.39	43.37	39.79	37.47	40.11
Fs	24.14	27.55	23.41	35.16	25.24	23.99	20.32	36.89	31.75	24.38	22.60	26.92	21.69
Relative proportions													
Ti	28.50	22.45	25.10	23.59	27.05	22.25	22.34	29.00	26.72	24.54	24.50	21.80	24.83
NaM_2	16.16	16.37	14.72	15.42	19.00	18.87	18.65	5.66	23.04	12.84	14.63	18.51	17.82
Al^{IV}	55.34	61.19	60.17	60.99	53.95	58.88	59.01	65.34	50.24	62.63	60.87	59.69	57.35
$Fe^{2+}/Fe^{2+} + Mg$	0.35	0.45	0.35	0.51	0.38	0.37	0.33	0.41	0.50	0.36	0.36	0.42	0.35

*This analysis of pigeonite is not acceptable using the tests of Papike and others (1974), but is included to illustrate its general composition.

Table A-4. Selected microprobe analyses of olivine

	Sill A	Sill B
Sample	M11521	M11566
Height (m)	10.7	21.6
Major oxides, weight percent		
SiO_2	31.6	32.0
TiO_2	0.63	0.19
Al_2O_3	0.2	0.00
FeO	59.6	53.7
MgO	9.4	15.2
CaO	0.21	0.19
MnO	0.73	0.44
Na_2O	0.03	0.00
K_2O	0.05	0.02
Total	102.4	101.7
Molecular proportions, O = 4		
Si	0.979	0.968
Ti	0.015	0.004
Al	0.008	0.000
Fe	1.543	1.356
Mg	0.432	0.682
Ca	0.007	0.006
Mn	0.019	0.011
Na	0.002	0.000
K	0.002	0.001
Total	3.007	3.028
Olivine components, mole percent		
Fo	21.9	33.5
Fa	78.1	66.5

Table A-5. Selected microprobe analyses of biotite, sill A

Sample	M11539		M11554		
Height (m)	38.1		131.4		
Major oxides, weight percent					
SiO_2	35.6	34.0	36.0	42.3	36.1
TiO_2	1.97	2.52	3.37	0.54	0.58
Al_2O_3	12.4	12.1	11.0	6.7	11.2
FeO	34.4	35.1	33.6	38.1	39.9
MgO	3.57	3.11	3.9	2.81	2.06
CaO	0.06	0.08	0.08	0.11	0.06
MnO	0.14	0.07	0.15	0.32	0.22
Na_2O	0.03	0.00	0.09	0.16	0.06
K_2O	8.33	8.40	8.21	4.47	7.29
Total	96.6	95.4	96.5	95.5	97.6
Tetrahedral cations, O + OH = 24					
Si	6.297	6.150	6.350	7.423	6.453
Al^{IV}	1.703	1.850	1.650	0.577	1.547
Total	8.000	8.000	8.000	8.000	8.000
Octahedral cations					
Al^{VI}	0.883	0.730	0.645	0.808	0.814
Ti	0.262	0.343	0.446	0.072	0.078
Fe	5.086	5.309	4.952	5.602	5.960
Mg	0.940	0.840	1.037	0.734	0.549
Mn	0.021	0.011	0.022	0.048	0.033
Total	7.192	7.233	7.102	7.264	7.434
Large cations					
Ca	0.011	0.016	0.015	0.020	0.012
Na	0.021	0.001	0.031	0.056	0.022
K	1.877	1.937	1.846	1.001	1.660
Total	1.909	1.954	1.892	1.077	1.694

Table A-6. Selected microprobe analyses of amphibole
[Amphibole names using the nomenclature of Leake (1978); Fe^{3+} estimated using methods of Papike and others (1974)]

Sample	Sill A M11554		Sill C M11625		Sill D M11631
Height (m)	131.4		1.5		2.1
	Ferro-edenite	Ferro-edenite	Ferro-edenite	Ferro-hornblende	Ferro-edenite
Major oxides, weight percent					
SiO_2	43.4	44.9	46.9	47.0	44.8
TiO_2	1.68	1.25	1.24	1.23	1.38
Al_2O_3	6.2	5.2	5.2	4.9	5.9
FeO	30.6	29.8	26.7	25.7	26.1
MgO	4.05	5.00	7.74	8.06	7.45
CaO	10.03	9.87	9.99	9.77	9.97
MnO	0.21	0.29	0.26	0.27	0.23
Na_2O	2.45	2.16	1.69	1.56	1.90
K_2O	0.95	0.80	0.68	0.55	0.77
Total	99.6	99.3	100.4	98.9	98.5
Tetrahedral T cations					
Si	6.844	7.033	7.093	7.155	6.940
Al	1.156	0.967	0.907	0.845	1.060
Total	8.000	8.000	8.000	8.000	8.000
Octahedral C cations					
Al	0.001	0.002	0.017	0.030	0.016
Ti	0.199	0.147	0.141	0.140	0.160
Fe^{3+}	0.006	0.012	0.097	0.175	0.096
Mg	0.951	1.167	1.746	1.829	1.719
Fe^{2+}	3.843	3.672	2.999	2.826	3.009
Total	5.000	5.000	5.000	5.000	5.000
Octahedral B cations					
Mn	0.028	0.039	0.033	0.034	0.030
Fe^{2+}	0.185	0.228	0.289	0.267	0.268
Ca	1.694	1.656	1.621	1.595	1.653
Na	0.093	0.077	0.057	0.104	0.049
Total	2.000	2.000	2.000	2.000	2.000
A cations					
Na	0.656	0.580	0.439	0.355	0.522
K	0.191	0.160	0.131	0.106	0.152
Total	0.847	0.740	0.570	0.462	0.674
$\frac{Mg}{Mg+Fe^{2+}}$	0.191	0.230	0.347	0.372	0.344